

# Autophagy determines osimertinib resistance through regulation of stem cell-like properties in EGFR-mutant lung cancer

Li Li<sup>1†</sup>, Yubo Wang<sup>1†</sup>, Lin Jiao<sup>1†</sup>, Caiyu Lin<sup>1</sup>, Conghua Lu<sup>1</sup>, Kejun Zhang<sup>2</sup>, Chen Hu<sup>1</sup>, Junyi Ye<sup>3</sup>, Dadong Zhang<sup>4</sup>, Mingxia Feng<sup>1</sup>, Yong He<sup>1\*</sup>

## Affiliations:

<sup>1</sup> Department of Respiratory Disease, Daping Hospital, Army Medical University, Chongqing 400042, China

<sup>2</sup> Department of Clinical Laboratory, Daping Hospital, Army Medical University, Chongqing 400042, China

<sup>3</sup> Burning Rock Biotech, Guangzhou 510300, China

<sup>4</sup> The Research and Development Institute of Precision Medicine, 3D Medicine Inc., Shanghai 201114, China.

<sup>†</sup> These authors contributed equally to this work.

**Running title:** Autophagy and osimertinib resistance

**\* Corresponding author:** Yong He, Department of Respiratory Disease, Daping Hospital, T Army Medical University, Chongqing 400042, China. Phone: 86-23-68757791; Fax: 86-23-68757791; E-mail: heyong8998@126.com

**Key words:** osimertinib, autophagy, drug resistance, stemness, beclin1

**Competing interests:** The authors disclosure no potential conflicts of interest.

## 27 ABSTRACT

28 Drug resistance to Osimertinib, a 3<sup>rd</sup>-generation EGFR-TKI is inevitable. Autophagy plays a  
 29 contradictory role in resistance of 1<sup>st</sup> and 2<sup>nd</sup> generation EGFR-TKI, and its significance in osimertinib  
 30 resistance is much less clear. We therefore investigated whether autophagy determines osimertinib  
 31 resistance. First, osimertinib induced autophagy to a much greater extent than that of gefitinib, and  
 32 autophagy inhibition further increased osimertinib efficacy. Next, enhanced autophagy was found in  
 33 osimertinib resistant cells and autophagy inhibition partially reversed osimertinib resistance. Enhanced  
 34 stem-cell like properties were found in resistant cells, and siRNA-knock down of *SOX2* or  
 35 *ALDH1A1* reversed osimertinib resistance. Of note, autophagy inhibition or siRNA-knock down of  
 36 Beclin-1 decreased expression of *SOX2* and *ALDH1A1* and stem-cell like properties. Next, autophagy  
 37 inhibition and osimertinib in combination effectively blocked tumor growth in xenografts, which was  
 38 associated with decreased autophagy and stem cell-like properties *in vivo*. Finally, enhanced autophagy  
 39 was found in lung cancer patients with resistance to osimertinib. In conclusion, the current study  
 40 delineates a previously unknown function of autophagy in determining osimertinib resistance through  
 41 promoting stem-cell like properties.

## 42 **Introduction**

43 Non-small-cell lung cancer (NSCLC) treatment has evolved dramatically in the last decade, from  
 44 the traditional “one-size-fits-all” chemotherapeutic approach to new targeted therapies against oncogenic  
 45 driver mutations. In NSCLC patients with EGFR-activating mutations, 1<sup>st</sup>-generation epidermal growth  
 46 factor receptor tyrosine kinase inhibitors (EGFR-TKIs) have become the standard first-line therapy with  
 47 dramatic therapeutic efficacy (Nguyen & Neal, 2012; Soria et al, 2012). However, acquired resistance is  
 48 unavoidable (Pao et al, 2005). Occurrence of a second EGFR mutation p.T790M in exon 20 represents  
 49 the most frequent mechanism of acquired resistance (Yu et al, 2013). Osimertinib (AZD9291) is a  
 50 3<sup>rd</sup>-generation irreversible EGFR-TKI with potent activities against T790M (Skoulidis &  
 51 Papadimitrakopoulou, 2017), and has shown significantly higher efficacy in T790M-positive advanced  
 52 NSCLC patients (Mok et al, 2017). Moreover, osimertinib showed efficacy superior to that of 1<sup>st</sup> or 2<sup>nd</sup>  
 53 generation EGFR-TKIs in the first-line treatment of EGFR mutation-positive advanced NSCLC (Soria et  
 54 al, 2018). However, it is very disappointing that acquired resistance to such a highly-effective and  
 55 low-toxicity drug will inevitably occur (Janne et al, 2015). Thus, innovative treatment strategies are  
 56 urgently needed to fully clarify the mechanisms of acquired resistance to osimertinib.

57 The mechanisms of osimertinib resistance are diverse and not fully understood. Emerging clinical  
 58 data suggest that the underlying mechanisms include other EGFR mutations, C797S and L798I, which  
 59 also prevent drug binding (Chabon et al, 2016; Thress et al, 2015), bypassing of MET or ERBB2  
 60 signaling activation (Kim et al, 2015; Mizuuchi et al, 2016; Ortiz-Cuaran et al, 2016; Planchard et al,  
 61 2015), or constitutive MAPK pathway activation by mutated KRAS or MEK (Eberlein et al, 2015).  
 62 Besides, amplification of EGFR wild-type alleles but not mutant alleles is sufficient to confer acquired  
 63 resistance to osimertinib (Nukaga et al, 2017). However, the majority of patients likely develop

64 resistance by as yet unknown mechanisms. Therefore, it is of great significance to investigate new  
65 treatment regimens which can reverse osimertinib resistance caused by diverse mechanism and enhance  
66 osimertinib efficacy.

67 Autophagy is an evolutionarily conserved catabolic process involving the degradation of  
68 cytoplasmic constituents, and the recycling of long-lived or aggregated proteins(Yu et al, 2017). In  
69 multiple tumor cells, autophagy is upregulated during adverse conditions, including chemoradiotherapy  
70 or a nutrient-deficient environment, promoting tumor cell survival; thus, autophagy may be considered a  
71 potential mechanism of drug resistance(2014; Auberger & Puissant, 2017; Chen et al, 2016b). In  
72 NSCLC treated with EGFR-TKI, autophagy is a double-edged sword contributing to both cell survival  
73 and death. Reduced autophagy was related to resistance to erlotinib therapy (Wei et al, 2013). On the  
74 other hand, several recent studies have shown that treatment of erlotinib or afatinib induced autophagy  
75 and inhibition of autophagy improves the anti-tumor activity of these drugs in lung adenocarcinoma (Hu  
76 et al, 2017; Wang et al, 2016). Moreover, the pro-cell survival and pro-cell death roles of autophagy can  
77 be switched by adding gefitinib at an early time of hypoxia or by re-activating EGFR at a later time of  
78 hypoxia in cancer cell lines (Chen et al, 2016a). Therefore, more works are needed to better understand  
79 the role of autophagy in EGFR-targeted therapy for NSCLCs. As a 3<sup>rd</sup> generation EGFR-TKI,  
80 osimertinib has a different chemical structure and different potential resistance mechanisms when  
81 compared to 1<sup>st</sup> or 2<sup>nd</sup> generation EGFR-TKI. Recently, in osimertinib-sensitive cells, osimertinib was  
82 found to induce autophagy (Tang et al, 2017). However, it is unknown whether the accumulated  
83 autophagy may induce osimertinib resistance, or whether inhibition of autophagy may restore  
84 osimertinib sensitivity.

85 Therefore, we preformed the current study to clarify the role of autophagy in osimertinib resistance

86 and the potential mechanisms. Since use of osimertinib in 1<sup>st</sup> or 2<sup>nd</sup> line may lead to different resistance  
 87 mechanisms, a series of cell lines were chosen to mimic the clinical usage of osimertinib, including  
 88 PC-9 cells (19del and sensitive to 1<sup>st</sup> generation EGFR-TKIs), PC-9GR cells (T790M+ with acquired  
 89 resistance to the 1<sup>st</sup> generation EGFR-TKI gefitinib), and H1975 cells (de novo T790M+ with primary  
 90 resistance to gefitinib), respectively. We first found that osimertinib treatment increased autophagy to a  
 91 much greater extent than that of gefitinib in osimertinib-sensitive cells, and autophagy inhibitors act  
 92 synergistically with osimertinib to inhibit cell growth. Next, we demonstrated that enhanced autophagy  
 93 was a common feature in osimertinib-resistant cells with heterogeneous mutations. Inhibition of  
 94 autophagy reversed osimertinib resistance. Mechanistically, beclin 1-mediated autophagy determined  
 95 osimertinib resistance through regulation of stem-cell like properties by upregulating Sox2 and ALDH1,  
 96 which indeed promote osimertinib resistance. Clinically, enhanced autophagy was also found in several  
 97 patients with resistance to osimertinib. These findings highlight the importance of beclin 1-mediated  
 98 autophagy in acquired resistance to osimertinib.

99

100

101

## 102 **Results**

### 103 **Enhanced autophagy lead to drug resistance in osimertinib-sensitive cells**

104 We first interrogated whether osimertinib treatment could induce autophagy and the role of  
 105 autophagy in osimertinib sensitivity. PC-9GR and PC-9 cells were treated with osimertinib, and then  
 106 exposed to cyto-ID green detection reagent that selectively labels accumulated autophagic vacuoles.  
 107 More pre-autophagosomes, autophagosomes, and autolysosomes were observed after osimertinib  
 108 treatment in PC-9GR and PC-9 cells. Increased LC3 II expression and decreased p62 expression were  
 109 also found in both cell lines after osimertinib treatment (Fig. 1A and B, Fig. S1). To further confirm  
 110 whether autophagy was induced after osimertinib treatment, we examined the autophagic flux in  
 111 osimertinib-treated PC-9 cells using MG132, a potent proteasome inhibitor. Result showed that LC3II  
 112 was further significantly increased in both cell lines under osimertinib plus MG132 combination  
 113 treatment compared to osimertinib alone, indicating that osimertinib induced high autophagic flux  
 114 (Fig. 1B, Fig. S2A). Interestingly, the level of osimertinib-induced autophagy was much higher than  
 115 that of gefitinib in PC-9 and PC-9GR cells (Fig. 1C, Fig. S2B). Considering previous reports that  
 116 autophagy play a complex role in gefitinib or erlotinib resistance, we next investigated whether the  
 117 highly elevated autophagy could affect osimertinib sensitivity. We observed that treatment with SP-1, a  
 118 specific and potent autophagy inhibitor, abolished osimertinib-induced autophagy increasement and  
 119 significantly increased osimertinib sensitivity in both cell lines, as determined by the MTT assay (Fig.  
 120 1D, Fig. S3). Similar results were obtained with two other autophagy inhibitors, 3-MA  
 121 (3-Methyladenine, a PI3K inhibitor) and CQ (chloroquine diphosphate salt, which inhibits the  
 122 integration of autophagosomes with lysosomes) (Fig. S4). The Ki67 incorporation assay revealed that  
 123 SP-1 combined with osimertinib resulted in a robust inhibition of cell proliferation in PC-9GR cells

(Fig. 1E). These results showed that osimertinib treatment induced autophagy in osimertinib-sensitive cells, and inhibition of autophagy increased osimertinib efficacy. We then investigated whether autophagy enhancement by rapamycin, the prototypic inhibitor of mammalian target of rapamycin (mTOR), could decrease osimertinib sensitivity. MTT assay showed that treatment with rapamycin resulted in decreased osimertinib sensitivity (Fig. 1F), and increased autophagy was confirmed by LC3II and p62 level alterations (Fig. 1G, Fig. S5). Taken together, we conclude that autophagy plays an important role in osimertinib sensitivity.

## **Generation of osimertinib-resistant cell lines**

In order to investigate whether autophagy plays a role in osimertinib resistance, osimertinib-resistant cell lines were established from PC-9GR cells, H1975 cells and PC-9 cells, respectively, using the single-colony selecting method. The origins of the parental cells were confirmed by the STR loci assay. The osimertinib-resistant cells (PC-9OR, PC-9GROR and H1975-OR cells) displayed similar morphologic features compared to parental cells (Fig. 2A, Fig. S6). Next, the MTT assay was performed to evaluate osimertinib resistance of the cell lines. As shown in Fig. 2B, they were all highly-resistant to osimertinib, with  $IC_{50}$  markedly elevated when compared with those of parental cells. Next, the long-term proliferation ability of the resistant cells was evaluated by colony formation assay. Under osimertinib pressure, colonies were found in osimertinib-resistant cells but not in parental cells (Fig. 2C, Fig. S7). These results indicated that these cell lines generated were highly resistant to osimertinib.

To clarify potential resistance mechanisms, DNA isolated from parental and resistant clones were subjected to whole exome sequencing. Several genetic alterations potentially relevant to osimertinib

resistance were identified (Fig. 2D). *EGFR* amplification and loss of T790M were identified in PC-9GROR3 cells, while *MET* amplification was found in all H1975-OR cells; *BRAF* amplification was detected in H1975-OR1 cells (Fig. 2D). However, no new mutations were found in PC-9OR cells. These results indicated that diverse mechanisms may exist in osimertinib resistance.

# **Enhanced autophagy in osimertinib-resistant cell lines determines resistance to osimertinib**

We next estimated autophagy levels in osimertinib-resistant cell lines. Increased numbers of accumulated autophagic vacuoles were found in these cells, as shown by fluorescence levels quantified using high-content imaging system (Fig. 3A, Fig. S8). Meanwhile, the protein levels of LC3II was upregulated and p62 was downregulated in PC-9GROR, PC-9OR and H1975-OR cells (Fig. 3B, Fig. S9). Next, we compared autophagy flux in parental and resistant cells. Under MG132 treatment, LC3 II level was highly increased in PC-9OR3 cells when compared with that of parental PC-9 cells (Fig.3 C, Fig. S10), indicating high autophagy flux in osimertinib-resistant cells. To further confirm autophagy completion, osimertinib-resistant cells and respective parental cells were assessed by transmission electron microscopy. Autolysosomes, which have a single limiting membrane and contain cytoplasmic/organellar materials at various stages of degradation, can be distinguished from autophagosomes (containing a double limiting membrane) by electron microscopy. More autolysosomes were found in PC-9GROR3, PC-9OR3 and H1975-OR3 cells, compared with respective parental cells (Fig. 2D). We further examined the relative levels of autophagic flux using mCherry-EGFP-LC3 in PC-9GR and PC-9GROR cells. After transfection, autophagosomes were shown as yellow punta (the combination of red and green fluorescence), and autolysosomes were shown as red punta (the extinction of EGFP in the acid environment of lysosomes). As shown in Figure E, both the number of yellow



autophagosomes and red autolysosomes (the extinction of EGFP in the acid environment of lysosomes) were increased in the PC-9GROR cells compared to PC-9GR cells. These observations indicated that the autophagic process was completed, rather than blocked at the fusion step.

Next, we examined the role of enhanced autophagy in osimertinib resistance through pharmacological inhibition of autophagy. SP-1 treatment suppressed autophagy in osimertinib-resistant PC-9GROR, PC-9OR and H1975-OR cells, as shown by decreased LC3 II levels and increased p62 amounts (Fig. S11, 12, 13). Importantly, treatment with SP-1 re-sensitized the resistant cells to osimertinib (Fig. 2E, Fig. S11, 12, 13). Another autophagy inhibitor CQ was also used to treat PC-9OR3 cells, and the cells became more sensitive to osimertinib (Fig. S14). Taken together, autophagy was enhanced in osimertinib-resistant cell lines, and inhibition of autophagy re-sensitized those cells to

# **osimertinib.Osimertinib-resistant cells have typical stem cell-like properties**

Cancer stem-like cells contribute to tumor heterogeneity and have been implicated in disease relapse and drug resistance (Yeo et al, 2016). To investigate the potential role of stem cell-like properties in osimertinib resistance, pulmosphere formation assay were performed. As expected, PC-9GROR, PC-9OR and H1975-OR cells displayed increased pulmospheres in terms of number and size, comparing to PC-9GR, PC-9 and H1975 cells, respectively (Fig. 4A, Fig. S15). Moreover, CD133 and CD44 are regarded as specific markers for stem-like cells in lung cancer (Nishino et al, 2017; Okudela et al, 2012; Sarvi et al, 2014). FACS analysis revealed that CD133- and CD44-positive cell populations in all osimertinib-resistant cells (PC-9OR, PC-9GROR and H1975-OR) was higher than their parental cells (Fig. 4B). In addition, it was reported that the transcription factor Sox2 and aldehyde dehydrogenase (ALDH) play major roles in stem-like NSCLC cells (Akunuru et al, 2012; Justilien et al, 2014; Sterlacci et al, 2014), either of which is thought to confer drug resistance to tyrosine kinase inhibitors(Dogan et al,

2014; Kim et al, 2014). In our study, higher Sox2 and ALDH1 levels were observed in osimertinib resistant cells when compared to their parental cells (Fig. 4C, Fig. S16). Taken together, these results demonstrated that osimertinib-resistant cells exhibited stem-cell like properties such as enhanced pulmosphere formation ability, higher CD133/CD44 enrichment as well as Sox2 and ALDH1 overexpression.

195

## 196 **Roles of Sox2 and ALDH1 in the maintenance of CSCs and osimertinib resistance**

197 To validate the roles of Sox2 and ALDH1 in stemness, small interfering RNAs targeting *SOX2* and  
 198 *ALDH1A1* respectively, were designed to investigated the sensitivity of PC-9OR3 cells to osimertinib.  
 199 First, MTT assay revealed that PC-9OR3 cells were more sensitive to osimertinib after knockdown of  
 200 either *SOX2* or *ALDH1A1* (Fig. 5A). Secondly, the pulmosphere formation assay showed that *SOX2* or  
 201 *ALDH1A1* knockdown significantly reduced the number and size of pulmospheres compared with  
 202 controls (Fig. 5B). Thirdly, colony formation assay demonstrated that *SOX2* or *ALDH1A1* knockdown  
 203 resulted in significantly decreased clone sizes, suggesting that Sox2 and ALDH1 were responsible for  
 204 the proliferation of resistant cells (Fig. 5B). Fourthly, PC-9OR3 cells transfected with either *SOX2* or  
 205 *ALDH1A1* siRNA displayed decreased CD133+ and CD44+ cell populations (Fig. 5C). These findings  
 206 indicated that Sox2 and ALDH1 might be essential for maintaining stemness and resistance to  
 207 osimertinib. In addition, ALDH1 protein levels decreased after silencing of *SOX2*, whereas no Sox2  
 208 protein levels change was observed after *ALDH1A1* knockdown (Fig. 5D, Fig. S17). These findings  
 209 demonstrated that the role of ALDH1 in maintaining stemness and osimertinib resistance might be  
 210 mediated by Sox2.

211

## 212 **Beclin 1-dependent, not Atg5-related autophagy maintains stem-like cell properties in** 213 **osimertinib-resistant cells**

214 We next investigated the mechanism of autophagy induced osimertinib resistance by maintaining stem  
215 cell-like properties. SP-1 treatment lead to smaller spheres PC-9OR3 cells, compared to control (Fig. 6A  
216 and Fig. S18). Flow cytometry also revealed that SP-1 resulted in decreased population rates of CD133  
217 and CD44 positive cells (Fig. 6B, Fig. S19). These findings indicated autophagy inhibition can decrease  
218 stem cell-like characteristics in osimertinib-resistant cells. In addition, we found that SP-1 treatment  
219 downregulated ALDH1 and Sox2 in osimertinib-resistant cells (PC-9OR1, 2, 3) (Fig. 6C, Fig. S20).  
220 Similar observations were obtained in PC-9GROR3 cells and H1975-OR3 cells (Fig. S21). These results  
221 demonstrated that autophagy inhibition can result in decreased stemness in osimertinib-resistant cells.

222 Atg5 is an essential gene in canonical macroautophagy, while the non-canonical autophagic  
223 pathway, which is independent of Atg5, has been reported (Honda et al, 2014; Ma et al, 2015). Next,  
224 we investigated whether Atg5-dependent autophagy maintains stem cell-like characteristics. Atg5 and  
225 phosphorylated beclin 1 (Ser 93) levels were increased in resistant cells, while total Beclin 1 expression  
226 remained unchanged (Fig. 6D and Fig.S22). Similar results were found in other osimertinib resistant  
227 cells (Fig. S23). Treatment with SP-1 resulted in decreased beclin 1 phosphorylation but not total beclin  
228 1 and Atg5 amounts (Fig. S24). We silenced Atg5 and beclin 1 by siRNAs to examine their effects on  
229 osimertinib resistance. Knockdown of beclin 1 resulted in enhanced sensitivity of PC-9OR3 cells to  
230 osimertinib, whereas Atg5 knockdown showed no remarkable effects (Fig. 6E, Fig. S25). Furthermore,  
231 colony and pulmosphere formation assays demonstrated that beclin 1, not Atg5, was essential for stem  
232 cell-like properties, as decreased colony formation and smaller pulmospheres were observed only in  
233 beclin 1 knockdown cells (Fig. 6F). In addition, siRNA targeting beclin 1 led to a significant decrease of

CD133/CD44-positive cells while siRNA targeting Atg5 showed no significant effects (Fig. 6G, Fig. S26).

Next, the effects of beclin 1 knockdown on Sox2 and ALDH1 protein levels were evaluated. Results showed that beclin 1 knockdown resulted in decreased Sox2 and ALDH1 protein amounts (Fig. 6H, Fig. S27), and beclin 1 knockdown also weakened the accumulation of Sox2 and ALDH1 proteins after the proteasome inhibitor MG132 treatment (Fig. 6I, Fig. S28). Interestingly, mRNA levels of *SOX2* and *ALDH1A1* were unchanged after beclin 1 knockdown (Fig. 6J). This suggested that beclin1, but not Atg5, might maintain stemness through preventing the protein degradation of Sox2 and ALDH in osimertinib-resistant cells.

#### **Autophagy inhibition enhances the anti-tumor activity of osimertinib in PC-9GR/mouse xenografts**

We next assessed whether combination of the autophagy inhibitor CQ and osimertinib is more effective in xenografts established with PC-9GR cells. Result showed that CQ treatment slightly reduced tumor growth in PC-9GR xenografts, and osimertinib alone resulted in significant tumor shrinkage. The combination of CQ and osimertinib can further inhibit tumor growth ( $P < 0.05$  compared with osimertinib alone; Fig. 7A). During the treatment, no overt weight loss was observed in mice treated with CQ and/or osimertinib (Fig. 7B). Collectively, these findings suggested that CQ enhanced the therapeutic efficacy of osimertinib *in vivo*.

Next we explored the mechanism of combined therapy which was more effective than monotherapy in PC-9GR xenografts. Immunohistochemical staining showed high expression of LC3 and low Sox2 levels in the combination group (Fig. 7C). Osimertinib treatment resulted in increased Beclin-1

phosphorylation, while the combination therapy decreased Beclin-1 and Sox2 phosphorylation (Fig. 7D). These findings suggested that CQ/osimertinib combination was associated with the inhibition of autophagy and stem cell like properties *in vivo*.

## **Enhanced autophagy was found in NSCLC patients with resistance to osimertinib**

Next, we investigated whether enhanced autophagy existed in NSCLC patients with resistance to osimertinib. A retrospective analysis was performed by enrolling 39 NSCLC patients who had developed drug resistance to osimertinib from August 2015 to Feb 2018 in our hospital. Prior to treatment of osimertinib, all these patients displayed resistance to 1st-generation EGFR-TKI and *EGFR* T790M mutation was detected in them. After osimertinib resistance, either plasma or tissue biopsies from these 39 patients were profiled by capture-based targeted ultra-deep sequencing. As shown in Fig. 8A, a series of potential resistance mechanisms were found, including EGFR C797S mutation, MET amplification, ERBB2 amplification, KRAS mutation, PI3K mutation, et al. Of note, 57% patients developed resistance with unknown mechanisms. We next examined LC3 expression in 5 patients with paired tumor tissue samples (before osimertinib treatment and after osimertinib resistance). Before osimertinib treatment, low LC3 expression was found in all 5 patients (Fig. 8B). After osimertinib resistance, elevated LC3 expression was found in 3 patients (Patient #1, 4 and 5). Overall mutation spectrum of the 5 patients was displayed in Fig. 8C. Of the 3 patients with increased LC3 expression after osimertinib resistance, EGFR C797S mutation was found in 1 patient, sensitive EGFR mutations were found in the other 2 patients. In the remaining 2 patients without LC3 level increasing, C-met amplification was identified. Taken together, these results indicate that enhanced autophagy exist in at least some NSCLC patients with resistance to osimertinib.

## 279 Discussion

280 Currently there is no effective approach to overcome acquired resistance to 3<sup>rd</sup>-generation  
 281 EGFR-TKI osimertinib. The current study demonstrated that enhanced autophagy not only induced drug  
 282 resistance in osimertinib-sensitive cells, but also was a general feature in osimertinib-resistant cells  
 283 which presents diverse and heterogeneous mutations. Autophagy inhibitors and osimertinib  
 284 synergistically inhibited the growth of both sensitive and resistant tumor cells. Enhanced stem-cell like  
 285 properties were found in osimertinib-resistant cells. Of note, beclin 1-mediated autophagy helped  
 286 maintain stem cell-like properties by upregulating Sox2 and ALDH1, which indeed facilitate osimertinib  
 287 resistance. CQ in combination with osimertinib significantly inhibited tumor growth in xenograft  
 288 experiments. Taken together, we have shown that pro-survival autophagy determines osimertinib  
 289 resistance through regulation of stem-cell like properties.

290 Role of autophagy in lung cancer targeted therapy is perplexing. In advanced lung adenocarcinoma  
 291 treated with gefitinib, ATG5 rs510532 and ATG10 rs10036653 genetic variations in autophagy core  
 292 genes are significantly associated with clinical outcomes (Yuan et al, 2017). Previously, reduced  
 293 autophagy was related to resistance to erlotinib therapy (Wei et al, 2013), and when autophagy is further  
 294 elevated by a treatment in addition to 2<sup>nd</sup> generation EGFR-TKI afatinib, it can induce autophagic cell  
 295 death (Lee et al, 2015). On the other hand, reports demonstrated that gefitinib and erlotinib induced  
 296 pro-cell survival autophagy in both sensitive and resistant cancer cells (Han et al, 2011; Sugita et al,  
 297 2015; Zou et al, 2013). Combining glucose deprivation and autophagy inhibitor could synergize and  
 298 overcome the acquired resistance against erlotinib (Ye et al, 2017). Taken together, the role of autophagy  
 299 in resistance to 1<sup>st</sup> and 2<sup>nd</sup> generation EGFR-TKI is contradictory. The chemical structure of osimertinib  
 300 is totally different from 1<sup>st</sup> and 2<sup>nd</sup> generation EGFR-TKI, and the role of autophagy in osimertinib

301 resistance is unknown.

302 In the current study, we found a striking difference between gefitinib and osimertinib-induced  
 303 autophagy. In gefitinib-resistant PC-9GR cells, the level of autophagy was only slightly higher than that  
 304 of parental PC-9 cells, while a much higher level of autophagy was found in osimertinib-resistant cell  
 305 lines than their parental cells. Moreover, in both PC-9 cells and PC-9GR cells, osimertinib induced  
 306 autophagy to a much greater extent than that of gefitinib. Significantly, inhibition of autophagy by  
 307 several inhibitors and si-RNAs *in vitro* resulted in enhanced osimertinib efficacy, and the combination of  
 308 CQ and osimertinib *in vivo* markedly decreased tumor growth than osimertinib alone. Clinically,  
 309 enhanced autophagy was found in several patients with resistance to osimertinib. These results indicate  
 310 that pro-cell survival autophagy leads to osimertinib resistance. Previously, activation of pro-survival  
 311 autophagy has been found in therapeutics of many cancer, and blockage of autophagy promotes cell  
 312 death (Amrein et al, 2011; Han et al, 2008; Lee et al, 2017). Inhibition of autophagy has been proposed  
 313 as a new approach to enhance efficacy of targeted therapy. For example, simultaneously targeting  
 314 Hedgehog signaling pathway and autophagy could overcome drug resistance of BCRABL-positive  
 315 chronic myeloid leukemia to imatinib (Zeng et al, 2015). Elevated autophagy activity contributes to the  
 316 enhanced tolerance to metabolic stresses of EGFRvIII-expressing cells in glioblastoma. Targeting this  
 317 survival mechanism abrogates this advantage and results in enhanced tumor cell killing (Jutten et al,  
 318 2018). Taken together, our results with those findings suggest that pro-cell survival autophagy plays an  
 319 important role in targeted therapy of cancer.

320 Targeting autophagy may be developed as a new approach to overcome osimertinib resistance  
 321 clinically. The current study established osimertinib-resistant cell lines from PC-9 cells, which have only  
 322 a sensitive EGFR mutation, and PC-9GR and H1975 cells, in which T790M is present. This choice of

cells reflected the clinical application of osimertinib in 1<sup>st</sup> or 2<sup>nd</sup> line settings. Besides, loss of T790M, EGFR amplification, Met amplification, and BRAF amplification were found in osimertinib-resistant cell lines, in line with the clinical situation that diverse mutations of known driver genes and unknown mechanisms faced by patients with osimertinib resistance (as shown in Fig. 8A). Interestingly, enhanced autophagy were found in all resistant cell lines and several patients with different potential resistance mechanisms to osimertinib, which indicates that autophagy inhibition may be effective in osimertinib-resistant patients with heterogeneous resistance mechanisms. In the current study, we found that CQ in combination with osimertinib *in vivo* markedly decreased tumor growth. CQ is an FDA approved drug used for malaria, rheumatoid arthritis, and other autoimmune diseases, and is very cheap with an established history of good tolerability. Therefore, CQ may be applied together with osimertinib clinically to enhance osimertinib efficacy or to overcome osimertinib resistance.

The underlying mechanism of how autophagy renders osimertinib resistance is unknown. The importance of stemness in tumor heterogeneity and the heterogeneity of resistance mechanisms found in osimertinib-resistant cell lines in the current study initiated us to investigate whether autophagy may regulate osimertinib resistance through regulation of stem cell-like properties. In fact, osimertinib-resistant cells exhibited stem-cell like properties of enhanced pulmosphere formation ability, high CD133/CD44 enrichment as well as Sox2 and ALDH1 overexpression. Moreover, siRNA knockdown of *SOX2* or *ALDH1A1* increased osimertinib sensitivity, decreased CD133+ and CD44+ populations as well as pulmosphere formation ability. These results indicate that Sox2-mediated ALDH1 expression was involved in maintaining stemness and conferring osimertinib resistance. Previously, stem cell-like features, including overexpression of putative stem cell markers ALDH1A1 and ABCB1, were observed in cells with acquired resistance to gefitinib or afatinib (Hashida et al, 2015; Shien et al,



2013). Also, stem cell-like characteristics were found in gefitinib-resistant cells, and knockdown of IL-8 led to loss of stem cell-like characteristics and enhanced gefitinib sensitivity (Liu et al, 2015). Therefore, our results, together with previous findings, indicate that enhanced stem cell-like properties mediate osimertinib resistance.

We next asked whether autophagy controls osimertinib resistance through regulation of stem cell-like properties. Previously, it was reported that autophagy suppresses hematopoietic stem cell metabolism by clearing active, healthy mitochondria to maintain stemness (Ho et al, 2017). Here, we addressed the importance of Beclin 1 in maintaining stem-cell like properties. We found that beclin 1 knockdown by siRNA resulted in complete suppression of stem-cell like properties (decreased formation of pulmospheres and reduced levels of the stem cell markers Sox2, ALDH1, and CD133/CD44), which are associated with osimertinib resistance. We also demonstrated that beclin 1 help prevent the protein degradation of Sox2 and ALDH to maintain stemness. These findings support a new physiological role for Beclin 1-dependent alternative macroautophagy in stem-like cell maintenance. Therefore, we hypothesized that Beclin 1 is beneficial for the maintenance of cancer stem-like cells by preventing the protein degradation of Sox2 and ALDH1.

Several studies have reported the role of autophagy in control of stemness of cancer cells. Autophagy maintains the stemness of ovarian cancer stem cells through regulation of FOXA2 (Peng et al, 2017), and inhibition of autophagy reduces chemoresistance and tumorigenic potential of ovarian cancer stem cells (Pagotto et al, 2017). Autophagy promotes the formation of vasculogenic mimicry by glioma stem cells through induction of KDR/VEGFR-2 activation (Wu et al, 2017). In acute myeloid leukemia stem cells, autophagy confers resistance to BET inhibitor JQ1 (Jang et al, 2017). Overall, these reports together with findings of the current study indicate that autophagy has a key role in maintenance

367 of stemness of cancer cells, which then contribute to therapeutic resistance.

368 Since autophagy is important for osimertinib resistance as shown above, it is reasonable to ask  
 369 which autophagy genes are involved. Canonical autophagy is mediated by evolutionarily conserved  
 370 autophagy-related genes (Atg genes), among which Atg5 is considered an essential component(Kim et  
 371 al, 2013). Recently, Atg5-independent autophagy was reported. Both canonical and Atg5-independent  
 372 non-canonical autophagic pathways have the same upstream autophagy initiation mechanism, regulated  
 373 by several autophagic proteins, including Unc-51-like kinase 1 (Ulk1) and Beclin 1. Although higher  
 374 expression levels of p-Beclin1 (Ser93) and Atg5 were observed in all osimertinib-resistant cell lines,  
 375 osimertinib resistance was indeed inhibited by beclin 1 knockdown but not Atg5 silencing. This study  
 376 firstly showed that Beclin 1-dependent and Atg5-independent alternative macroautophagy mediated  
 377 osimertinib resistance.

378

## 379 **Conclusion**

380 In summary, this study delineates a previously unknown function of autophagy in promoting stemness  
 381 and osimertinib resistance. Such findings are critical for devising a potential therapeutic strategy to  
 382 overcome osimertinib resistance. In the future, more clinical work are needed to study whether  
 383 autophagy level was enhanced in osimertinib-resistant patients and to test the efficacy of autophagy  
 384 inhibition in combination with osimertinib in EGFR-mutant patients.

385

386

# **Materials and Methods**

## **Cell lines**

PC-9 cells and gefitinib-resistant PC-9GR cells were generously provided by Prof. J. Xu and Dr. M. Liu (Guangzhou Medical University, China). H1975 cells were from the American Type Culture Collection (ATCC). To establish osimertinib-resistant cell lines, the parental cells were treated with osimertinib at the concentration of IC<sub>50</sub> for 2 weeks, with higher drug levels for another 3 weeks. The latter dosage was sufficient to kill all parental cells. When resistant clones were visible, the cells were diluted to a single cell per well, and continuous culture was performed in presence of osimertinib. All cells were cultured in RPMI-1640 (Hyclone) with Earle's salts, supplemented with 10% FBS (Gibco), 2 mmol/L L-glutamine (Gibco), 100U/ml penicillin (HyClone), and 100μg/mL streptomycin (Hyclone) at 37°C, with 5% CO<sub>2</sub> and 90% humidity.

## **Reagents**

Osimertinib (TAGRISSO) was obtained from Astra Zeneca. Spautin-1 (S7888), 3-Methyladenine (S2767) and rapamycin (S1039) were purchased from Selleck. Cycloheximide (C6628) was purchased from Sigma-Aldrich, and cycloheximide (HY-12320) from MedChem Express. Anti-LC3II (#12741S), SQSTM1/p62 (#8025S), Atg5 (#9980S), Beclin 1 (#3495S), phospho-(Ser93)-beclin1 (#14717S), Sox2 (#3579S), ALDH1A1 (#36671S), GAPDH (#2118S) antibodies were from Cell Signaling Technology.

## **Cell growth assays**

The MTT cell proliferation assay was performed as previously described(Yao et al, 2010). Briefly, 2×10<sup>3</sup> cells/well were seeded in 96-well plates and treated with osimertinib or dimethyl sulfoxide

(DMSO) 24 hours later. Absorbance was measured 72 hours after treatment. All experiments were repeated for at least three times. Cell proliferation was also assessed by the Ki67 incorporation assay with a Ki67 labeling and detection kit (BM2889, Boster). Briefly, cells were treated with osimertinib for 48h, incubated for 6h with Ki67 (1:200 dilution), and fixed. Cells were counterstained with 4', 6-diamidino-2-phenylindole (DAPI) and observed under a fluorescence microscope.

414

### 415 **Colony-formation assay**

Briefly, 500 cells were resuspended in culture medium and seeded in six-well plates. After 14 days of culture, the cells were fixed with 4% paraformaldehyde and stained with 0.1% crystal violet. Colonies with a diameter greater than 1 mm were counted. Triplicate samples were used in the experiment.

419

### 420 **Transmission electron microscopy (TEM)**

The cells were pre-fixed with 2.5% glutaraldehyde in 0.1M PBS (pH 7.4) for 2h at room temperature, and post-fixed with 1% osmium tetroxide for 2h. The samples were then dehydrated in increasing concentrations of ethanol (50%, 70% and 100%) and acetone, and finally embedded in Araldite. Fifty to sixty nanometer sections were cut on a LKB-I ultramicrotome and transferred to copper grids, post-stained with uranyl acetate and lead citrate, and examined by Gatan JEM-1400 plus transmission electron microscopy.

427

### 428 **Whole-exome sequencing**

Whole-exome sequencing libraries were prepared with 3 mg DNA. Exomes were captured using the NimbleGen SeqCap Non-Standard Material 110823-HG19-BEx-L2R-D03-EZ for whole exome

430

sequencing, and libraries were hybridized to custom-designed biotinylated oligonucleotide probes (Roche NimbleGen, USA) covering the target region sequence for target-capture sequencing. DNA sequencing was carried out on a HiSeq Sequencing System (Illumina, CA) with 2×151-bp and 2×76-bp paired-end reads for WES and target-capture sequencing, respectively. Raw sequencing reads were filtered to obtain clean reads, which were then aligned to human genome assembly HG19 with Burrows-Wheeler Aligner (BWA) (Newman et al, 2016). Reads with multiple mapping loci in the genome, and those with more than three mismatches, more than one gap, or a gap of more than 20 base long were removed. Reads harboring an Indel within 5 bp of the fragment ends were removed. Duplicated reads derived from PCR amplification were marked with Picard tools (<http://broadinstitute.github.io/picard/>). Local realignments and base-quality recalibrations were performed with the GATK software (<https://www.broadinstitute.org/gatk/>).

### **Measurement of autophagic activity and autophagy flux**

Autophagic activity was monitored with the Cell-ID Green Autophagy Detection Kit (Enzo Life Sciences, France). The Cell-ID Green autophagy dye serves as a selective marker of autolysosomes and early autophagic compartments. Cells were trypsinized, washed with Assay Buffer, and incubated with Cell-ID Green Detection Reagent for 30 min at room temperature, according to the manufacturer's instructions. Afterwards, 10,000 events/sample were analyzed by fluorescence microscopy. The 24-well plates were imaged on an ImageXpress Micro (Molecular Devices) high-throughput imager. Image analysis was performed with the MetaXpress software.

To measure autophagy flux, pBABE-EGFP-mCherry-MAP1LC3B (22418, deposited by Jayanta Debnath) plasmid was obtained from Addgene and detailed methods was described previously (Gump et

al, 2014). PC-9GR and PC-9GROR cells were transduced with this plasmid for 6h and then replaced fresh media. We used ImageXpress Micro XLS Widefield High-Content screening System to automatic scanning the fluorescent dots of autophagosomes labeled mCherry-EGFP-LC3 after an interval 12h., and the final time point was 72h. Autophagic flux was determined by the yellow punta (the combination of red and green fluorescence), and red punta (the extinction of EGFP in the acid environment of lysosomes).

## Western blot

Cells harvested by scraping were washed twice with PBS and lysed for 30 min at 4°C in RIPA buffer (Sigma-Aldrich, France). After centrifugation at 12000×g for 15 min at 4°C, the protein content was determined by the BCA assay. Equal amounts of protein were submitted to gel electrophoresis for 2h at 110 V, followed by transfer onto PVDF membranes (90 min, 200 mA) (Roche, Switzerland). Membranes were blocked with 5% bovine serum albumin (BSA) for 1h at room temperature and incubated overnight at 4°C with primary antibodies. Subsequently, the membranes were washed and incubated with 0.02 µg/ml horseradish peroxidase (HRP)-conjugated goat anti-rabbit or anti-mouse IgG (Cell Signaling Technology, USA) for 1h, and visualized with ChemiDoc Touch System (Bio-Rad, USA).

## Pulmosphere formation assay

For tumor pulmosphere formation,  $1 \times 10^3$  tumor cells were seeded in non-adhesive 6-well plates. One week after seeding, cell spheres characterized by tight, spherical, non-adherent colonies > 90µm in diameter were observed. All experiments were repeated at least three times.

475

## 476 **Flow cytometry**

477 For CD133 and CD44 staining,  $10^6$  cells were incubated with 10 $\mu$ l of each anti-CD133-PE (AC133  
478 clone; Miltenyi Biotech) and anti-CD44-FITC (REA690 clone; Miltenyi Biotech) antibodies diluted in  
479 100 $\mu$ l of staining solution for 15 min at 4°C. Then, 400 $\mu$ l buffer was added, and samples were analyzed  
480 with the CytExpert software (Beckman Coulter, USA).

481

## 482 **siRNA Transfection**

483 Small interfering RNAs (siRNAs) were synthesized by Shanghai GenePharma Co., Ltd. (Shanghai,  
484 China). For efficacy evaluation, 80 pmol siRNA and negative control siRNA (siNC), respectively, were  
485 transfected into PC-9OR cells cultured in 6-well plates using Lipofectamine RNAiMAX, following the  
486 manufacturer's instructions. At 72h post-transfection, knockdown efficiency was determined by  
487 examining endogenous expression by Western blot.

488

## 489 **Quantitative RT-PCR**

490 Total RNA was isolated from cultured cells with TRIzol reagent (#15596026, Thermo Scientific, USA),  
491 and subjected to reverse transcription with PrimeScript RT reagent Kit containing gDNA Eraser  
492 (TAKARA, RR047A), according to the manufacturer's protocol. Quantitative RT-PCR was performed  
493 with fluorescent SYBR Green on a CFX96 Touch System (Bio-Rad, USA). Human GAPDH was used to  
494 normalize input cDNA.

495

## 496 **Xenografts**

Methods for xenograft implantation were described previously (Li et al, 2014). All animal protocols were approved by the Ethics Committee of the Third Military Medical University. Briefly,  $2 \times 10^6$  PC-9GR cells were injected subcutaneously into the back, next to the left forelimb of 6-week-old female BALB/c A-nu mice (Laboratory Animal Center of Third Military Medical University, Chongqing, China), which all developed tumors of  $\sim 30 \text{ mm}^3$  within 5 to 7 days. The mice were then randomly assigned to 4 groups (8 mice/group), and treated with CQ (100 mg/L), osimertinib (20 mg/L), combined CQ and osimertinib, and drinking water (vehicle). The tumor volume was calculated as  $(\text{length} \times \text{width}^2)/2$ , and measured twice a week. The animals were maintained in individual ventilated cages in compliance with institutional guidelines. The animals were monitored for 8 weeks until euthanasia. For immunohistochemistry assay, tumor bearing mice in each group were sacrificed after 4 weeks of drug administration, and tumors were harvested, fixed with 4% paraformaldehyde, and paraffin embedded.

## **Immunohistochemistry**

For immunohistochemistry, tumor sections were fixed with 4% paraformaldehyde overnight, paraffin embedded, sectioned, and stained with primary antibodies raised against Sox2 and LC3 (1:200). Sample scoring was performed by the H-score method that combines immunoreaction intensity and the percentage of tumor cells stained.

## **Patient information, sample preparation and NGS sequencing**

A retrospective investigation was performed by profiling plasma or tissue biopsies from 39 patients with acquired resistance to osimertinib using NGS. This study was approved by the Institutional Review Board of Daping Hospital, Army military medical university. All patients were provided informed



consent to this study and gave permission to the entire study. Disease progression was confirmed in each patient according to Recist 1.1 criterion. Tissue DNA was extracted using QIAamp DNA FFPE tissue kit (Qiagen) according to manufacturer's instructions. Circulating cell-free DNA was recovered from 4 to 5 ml of plasma using the QIAamp Circulating Nucleic Acid kit by Qiagen (Valencia, California, US). DNA shearing was performed using Covaris M220. End repair and A tailing was followed by adaptor ligation. The ligated fragments with size of 200-400 bp were selected by beads (Agencourt AMPure XP Kit, Beckman Coulter, California, US), hybridized with probe baits, selected by magnetic beads and amplified by PCR. Indexed samples were sequenced on Nextseq500 sequencer (Illumina, Inc., USA) with pair-end reads.

528

## 529 **Statistical analysis**

Statistical analysis was performed by GraphPad Prism 5 and the data were presented as mean  $\pm$  S.E.M. The two-tailed Student's t test was used to compare multiple sets of data.  $P < 0.05$  was considered to be statistically remarkable.

533

534 **Acknowledgments**

535 We thank Dr. Raffaella Sordella from Cold Spring Harbor Laboratory for kindly providing the valuable  
 536 cell lines used in the current study. We thank Prof. Xiang Xu and Prof. Xueqing Xu (both from Army  
 537 Medical University) for their kind advice about design of the study. This work was supported by the  
 538 Natural Science Foundation of China (81672284, 81472189, 81672287, 81702288 and 81702291) and a  
 539 foundation for PLA Young Scientists (16QNP106).

540

541 **Competing interests:** The authors disclosure no potential conflicts of interest.

542

## 543 **References**

- 544 (2014) BRAF inhibitor resistance can be overcome by blocking autophagy. *Cancer Discov* **4**: OF10
- 545
- 546 Akunuru S, James Zhai Q, Zheng Y (2012) Non-small cell lung cancer stem/progenitor cells are
- 547 enriched in multiple distinct phenotypic subpopulations and exhibit plasticity. *Cell death & disease* **3**:
- 548 e352
- 549
- 550 Amrein L, Soulieres D, Johnston JB, Aloyz R (2011) p53 and autophagy contribute to dasatinib
- 551 resistance in primary CLL lymphocytes. *Leuk Res* **35**: 99-102
- 552
- 553 Auberger P, Puissant A (2017) Autophagy, a key mechanism of oncogenesis and resistance in leukemia.
- 554 *Blood* **129**: 547-552
- 555
- 556 Chabon JJ, Simmons AD, Lovejoy AF, Esfahani MS, Newman AM, Haringsma HJ, Kurtz DM, Stehr H,
- 557 Scherer F, Karlovich CA, Harding TC, Durkin KA, Otterson GA, Purcell WT, Camidge DR, Goldman
- 558 JW, Sequist LV, Piotrowska Z, Wakelee HA, Neal JW, Alizadeh AA, Diehn M (2016) Circulating tumour
- 559 DNA profiling reveals heterogeneity of EGFR inhibitor resistance mechanisms in lung cancer patients.
- 560 *Nature communications* **7**: 11815
- 561
- 562 Chen Y, Henson ES, Xiao W, Huang D, McMillan-Ward EM, Israels SJ, Gibson SB (2016a) Tyrosine
- 563 kinase receptor EGFR regulates the switch in cancer cells between cell survival and cell death induced
- 564 by autophagy in hypoxia. *Autophagy* **12**: 1029-1046

565

566 Chen Z, Teo AE, McCarty N (2016b) ROS-Induced CXCR4 Signaling Regulates Mantle Cell  
567 Lymphoma (MCL) Cell Survival and Drug Resistance in the Bone Marrow Microenvironment via  
568 Autophagy. *Clinical cancer research : an official journal of the American Association for Cancer*  
569 *Research* **22**: 187-199

570

571 Dogan I, Kawabata S, Bergbower E, Gills JJ, Ekmekci A, Wilson W, 3rd, Rudin CM, Dennis PA (2014)  
572 SOX2 expression is an early event in a murine model of EGFR mutant lung cancer and promotes  
573 proliferation of a subset of EGFR mutant lung adenocarcinoma cell lines. *Lung cancer* **85**: 1-6

574

575 Eberlein CA, Stetson D, Markovets AA, Al-Kadhimi KJ, Lai Z, Fisher PR, Meador CB, Spitzler P,  
576 Ichihara E, Ross SJ, Ahdesmaki MJ, Ahmed A, Ratcliffe LE, O'Brien EL, Barnes CH, Brown H, Smith  
577 PD, Dry JR, Beran G, Thress KS, Dougherty B, Pao W, Cross DA (2015) Acquired Resistance to the  
578 Mutant-Selective EGFR Inhibitor AZD9291 Is Associated with Increased Dependence on RAS  
579 Signaling in Preclinical Models. *Cancer research* **75**: 2489-2500

580

581 Gump JM, Staskiewicz L, Morgan MJ, Bamberg A, Riches DW, Thorburn A (2014) Autophagy variation  
582 within a cell population determines cell fate through selective degradation of Fap-1. *Nat Cell Biol* **16**:  
583 47-54

584

585 Han J, Hou W, Goldstein LA, Lu C, Stolz DB, Yin XM, Rabinowich H (2008) Involvement of protective  
586 autophagy in TRAIL resistance of apoptosis-defective tumor cells. *The Journal of biological chemistry*

587 **283:** 19665-19677

588

589 Han W, Pan H, Chen Y, Sun J, Wang Y, Li J, Ge W, Feng L, Lin X, Wang X, Wang X, Jin H (2011)

590 EGFR tyrosine kinase inhibitors activate autophagy as a cytoprotective response in human lung cancer

591 cells. *PloS one* **6:** e18691

592

593 Hashida S, Yamamoto H, Shien K, Miyoshi Y, Ohtsuka T, Suzawa K, Watanabe M, Maki Y, Soh J,

594 Asano H, Tsukuda K, Miyoshi S, Toyooka S (2015) Acquisition of cancer stem cell-like properties in

595 non-small cell lung cancer with acquired resistance to afatinib. *Cancer science* **106:** 1377-1384

596

597 Ho TT, Warr MR, Adelman ER, Lansinger OM, Flach J, Verovskaya EV, Figueroa ME, Passegue E

598 (2017) Autophagy maintains the metabolism and function of young and old stem cells. *Nature* **543:**

599 205-210

600

601 Honda S, Arakawa S, Nishida Y, Yamaguchi H, Ishii E, Shimizu S (2014) Ulk1-mediated

602 Atg5-independent macroautophagy mediates elimination of mitochondria from embryonic reticulocytes.

603 *Nature communications* **5:** 4004

604

605 Hu X, Shi S, Wang H, Yu X, Wang Q, Jiang S, Ju D, Ye L, Feng M (2017) Blocking autophagy improves

606 the anti-tumor activity of afatinib in lung adenocarcinoma with activating EGFR mutations in vitro and

607 in vivo. *Scientific reports* **7:** 4559

608

609 Jang JE, Eom JI, Jeung HK, Cheong JW, Lee JY, Kim JS, Min YH (2017) AMPK-ULK1-Mediated  
610 Autophagy Confers Resistance to BET Inhibitor JQ1 in Acute Myeloid Leukemia Stem Cells. *Clinical*  
611 *cancer research : an official journal of the American Association for Cancer Research* **23**: 2781-2794  
612

613 Janne PA, Yang JC, Kim DW, Planchard D, Ohe Y, Ramalingam SS, Ahn MJ, Kim SW, Su WC, Horn L,  
614 Haggstrom D, Felip E, Kim JH, Frewer P, Cantarini M, Brown KH, Dickinson PA, Ghiorghiu S, Ranson  
615 M (2015) AZD9291 in EGFR inhibitor-resistant non-small-cell lung cancer. *The New England journal of*  
616 *medicine* **372**: 1689-1699  
617

618 Justilien V, Walsh MP, Ali SA, Thompson EA, Murray NR, Fields AP (2014) The PRKCI and SOX2  
619 oncogenes are coamplified and cooperate to activate Hedgehog signaling in lung squamous cell  
620 carcinoma. *Cancer Cell* **25**: 139-151  
621

622 Jutten B, Keulers TG, Peeters HJM, Schaaf MBE, Savelkoul KGM, Compter I, Clarijs R, Schijns O,  
623 Ackermans L, Teernstra OPM, Zonneveld MI, Colaris RME, Dubois L, Vooijs MA, Bussink J, Sotelo J,  
624 Theys J, Lammering G, Rouschop KMA (2018) EGFRvIII expression triggers a metabolic dependency  
625 and therapeutic vulnerability sensitive to autophagy inhibition. *Autophagy*: 1-13  
626

627 Kim IG, Kim SY, Choi SI, Lee JH, Kim KC, Cho EW (2014) Fibulin-3-mediated inhibition of  
628 epithelial-to-mesenchymal transition and self-renewal of ALDH+ lung cancer stem cells through IGF1R  
629 signaling. *Oncogene* **33**: 3908-3917  
630

631 Kim J, Kim YC, Fang C, Russell RC, Kim JH, Fan W, Liu R, Zhong Q, Guan KL (2013) Differential  
632 regulation of distinct Vps34 complexes by AMPK in nutrient stress and autophagy. *Cell* **152**: 290-303  
633

634 Kim TM, Song A, Kim DW, Kim S, Ahn YO, Keam B, Jeon YK, Lee SH, Chung DH, Heo DS (2015)  
635 Mechanisms of Acquired Resistance to AZD9291: A Mutation-Selective, Irreversible EGFR Inhibitor.  
636 *Journal of thoracic oncology : official publication of the International Association for the Study of Lung*  
637 *Cancer* **10**: 1736-1744  
638

639 Lee MH, Koh D, Na H, Ka NL, Kim S, Kim HJ, Hong S, Shin YK, Seong JK, Lee MO (2017) MTA1 is  
640 a novel regulator of autophagy that induces tamoxifen resistance in breast cancer cells. *Autophagy*: 0  
641

642 Lee TG, Jeong EH, Kim SY, Kim HR, Kim CH (2015) The combination of irreversible EGFR TKIs and  
643 SAHA induces apoptosis and autophagy-mediated cell death to overcome acquired resistance in EGFR  
644 T790M-mutated lung cancer. *International journal of cancer* **136**: 2717-2729  
645

646 Li L, Han R, Xiao H, Lin C, Wang Y, Liu H, Li K, Chen H, Sun F, Yang Z, Jiang J, He Y (2014)  
647 Metformin sensitizes EGFR-TKI-resistant human lung cancer cells in vitro and in vivo through  
648 inhibition of IL-6 signaling and EMT reversal. *Clinical cancer research : an official journal of the*  
649 *American Association for Cancer Research* **20**: 2714-2726  
650

651 Liu YN, Chang TH, Tsai MF, Wu SG, Tsai TH, Chen HY, Yu SL, Yang JC, Shih JY (2015) IL-8 confers  
652 resistance to EGFR inhibitors by inducing stem cell properties in lung cancer. *Oncotarget* **6**:

10415-10431

Ma T, Li J, Xu Y, Yu C, Xu T, Wang H, Liu K, Cao N, Nie BM, Zhu SY, Xu S, Li K, Wei WG, Wu Y, Guan KL, Ding S (2015) Atg5-independent autophagy regulates mitochondrial clearance and is essential for iPSC reprogramming. *Nat Cell Biol* **17**: 1379-1387

Mizuuchi H, Suda K, Murakami I, Sakai K, Sato K, Kobayashi Y, Shimoji M, Chiba M, Sesumi Y, Tomizawa K, Takemoto T, Sekido Y, Nishio K, Mitsudomi T (2016) Oncogene swap as a novel mechanism of acquired resistance to epidermal growth factor receptor-tyrosine kinase inhibitor in lung cancer. *Cancer science* **107**: 461-468

Mok TS, Wu YL, Ahn MJ, Garassino MC, Kim HR, Ramalingam SS, Shepherd FA, He Y, Akamatsu H, Theelen WS, Lee CK, Sebastian M, Templeton A, Mann H, Marotti M, Ghiorghiu S, Papadimitrakopoulou VA, Investigators A (2017) Osimertinib or Platinum-Pemetrexed in EGFR T790M-Positive Lung Cancer. *The New England journal of medicine* **376**: 629-640

Newman AM, Lovejoy AF, Klass DM, Kurtz DM, Chabon JJ, Scherer F, Stehr H, Liu CL, Bratman SV, Say C, Zhou L, Carter JN, West RB, Sledge GW, Shrager JB, Loo BW, Jr., Neal JW, Wakelee HA, Diehn M, Alizadeh AA (2016) Integrated digital error suppression for improved detection of circulating tumor DNA. *Nature biotechnology* **34**: 547-555

Nguyen KS, Neal JW (2012) First-line treatment of EGFR-mutant non-small-cell lung cancer: the role



of erlotinib and other tyrosine kinase inhibitors. *Biologics : targets & therapy* **6**: 337-345

Nishino M, Ozaki M, Hegab AE, Hamamoto J, Kagawa S, Arai D, Yasuda H, Naoki K, Soejima K, Saya H, Betsuyaku T (2017) Variant CD44 expression is enriching for a cell population with cancer stem cell-like characteristics in human lung adenocarcinoma. *Journal of Cancer* **8**: 1774-1785

Nukaga S, Yasuda H, Tsuchihara K, Hamamoto J, Masuzawa K, Kawada I, Naoki K, Matsumoto S, Mimaki S, Ikemura S, Goto K, Betsuyaku T, Soejima K (2017) Amplification of EGFR Wild-Type Alleles in Non-Small Cell Lung Cancer Cells Confers Acquired Resistance to Mutation-Selective EGFR Tyrosine Kinase Inhibitors. *Cancer research* **77**: 2078-2089

Okudela K, Woo T, Mitsui H, Tajiri M, Masuda M, Ohashi K (2012) Expression of the potential cancer stem cell markers, CD133, CD44, ALDH1, and beta-catenin, in primary lung adenocarcinoma--their prognostic significance. *Pathol Int* **62**: 792-801

Ortiz-Cuaran S, Scheffler M, Plenker D, Dahmen L, Scheel AH, Fernandez-Cuesta L, Meder L, Lovly CM, Persigehl T, Merkelbach-Bruse S, Bos M, Michels S, Fischer R, Albus K, Konig K, Schildhaus HU, Fassunke J, Ihle MA, Pasternack H, Heydt C, Becker C, Altmuller J, Ji H, Muller C, Florin A, Heuckmann JM, Nuernberg P, Ansen S, Heukamp LC, Berg J, Pao W, Peifer M, Buettner R, Wolf J, Thomas RK, Sos ML (2016) Heterogeneous Mechanisms of Primary and Acquired Resistance to Third-Generation EGFR Inhibitors. *Clinical cancer research : an official journal of the American Association for Cancer Research* **22**: 4837-4847

697

698 Pagotto A, Pilotto G, Mazzoldi EL, Nicoletto MO, Frezzini S, Pasto A, Amadori A (2017) Autophagy  
699 inhibition reduces chemoresistance and tumorigenic potential of human ovarian cancer stem cells. *Cell*  
700 *death & disease* **8**: e2943

701

702 Pao W, Miller VA, Politi KA, Riely GJ, Somwar R, Zakowski MF, Kris MG, Varmus H (2005) Acquired  
703 resistance of lung adenocarcinomas to gefitinib or erlotinib is associated with a second mutation in the  
704 EGFR kinase domain. *PLoS medicine* **2**: e73

705

706 Peng Q, Qin J, Zhang Y, Cheng X, Wang X, Lu W, Xie X, Zhang S (2017) Autophagy maintains the  
707 stemness of ovarian cancer stem cells by FOXA2. *Journal of experimental & clinical cancer research* :  
708 *CR* **36**: 171

709

710 Planchard D, Loriot Y, Andre F, Gobert A, Auger N, Lacroix L, Soria JC (2015) EGFR-independent  
711 mechanisms of acquired resistance to AZD9291 in EGFR T790M-positive NSCLC patients. *Annals of*  
712 *oncology : official journal of the European Society for Medical Oncology* **26**: 2073-2078

713

714 Sarvi S, Mackinnon AC, Avlonitis N, Bradley M, Rintoul RC, Rassl DM, Wang W, Forbes SJ, Gregory  
715 CD, Sethi T (2014) CD133+ cancer stem-like cells in small cell lung cancer are highly tumorigenic and  
716 chemoresistant but sensitive to a novel neuropeptide antagonist. *Cancer research* **74**: 1554-1565

717

718 Shien K, Toyooka S, Yamamoto H, Soh J, Jida M, Thu KL, Hashida S, Maki Y, Ichihara E, Asano H,

719 Tsukuda K, Takigawa N, Kiura K, Gazdar AF, Lam WL, Miyoshi S (2013) Acquired resistance to EGFR  
720 inhibitors is associated with a manifestation of stem cell-like properties in cancer cells. *Cancer research*  
721 **73**: 3051-3061

722

723 Skoulidis F, Papadimitrakopoulou VA (2017) Targeting the Gatekeeper: Osimertinib in EGFR T790M  
724 Mutation-Positive Non-Small Cell Lung Cancer. *Clinical cancer research : an official journal of the*  
725 *American Association for Cancer Research* **23**: 618-622

726

727 Soria JC, Mok TS, Cappuzzo F, Janne PA (2012) EGFR-mutated oncogene-addicted non-small cell lung  
728 cancer: current trends and future prospects. *Cancer treatment reviews* **38**: 416-430

729

730 Soria JC, Ohe Y, Vansteenkiste J, Reungwetwattana T, Chewaskulyong B, Lee KH, Dechaphunkul A,  
731 Imamura F, Nogami N, Kurata T, Okamoto I, Zhou C, Cho BC, Cheng Y, Cho EK, Voon PJ, Planchard  
732 D, Su WC, Gray JE, Lee SM, Hodge R, Marotti M, Rukazenzov Y, Ramalingam SS, Investigators F  
733 (2018) Osimertinib in Untreated EGFR-Mutated Advanced Non-Small-Cell Lung Cancer. *The New*  
734 *England journal of medicine* **378**: 113-125

735

736 Sterlacci W, Savic S, Fiegl M, Obermann E, Tzankov A (2014) Putative stem cell markers in  
737 non-small-cell lung cancer: a clinicopathologic characterization. *Journal of thoracic oncology : official*  
738 *publication of the International Association for the Study of Lung Cancer* **9**: 41-49

739

740 Sugita S, Ito K, Yamashiro Y, Moriya S, Che XF, Yokoyama T, Hiramoto M, Miyazawa K (2015)

741 EGFR-independent autophagy induction with gefitinib and enhancement of its cytotoxic effect by  
742 targeting autophagy with clarithromycin in non-small cell lung cancer cells. *Biochem Biophys Res*  
743 *Commun* **461**: 28-34

744

745 Tang ZH, Cao WX, Su MX, Chen X, Lu JJ (2017) Osimertinib induces autophagy and apoptosis via  
746 reactive oxygen species generation in non-small cell lung cancer cells. *Toxicol Appl Pharmacol* **321**:  
747 18-26

748

749 Thress KS, Paweletz CP, Felip E, Cho BC, Stetson D, Dougherty B, Lai Z, Markovets A, Vivancos A,  
750 Kuang Y, Ercan D, Matthews SE, Cantarini M, Barrett JC, Janne PA, Oxnard GR (2015) Acquired  
751 EGFR C797S mutation mediates resistance to AZD9291 in non-small cell lung cancer harboring EGFR  
752 T790M. *Nature medicine* **21**: 560-562

753

754 Wang Z, Du T, Dong X, Li Z, Wu G, Zhang R (2016) Autophagy inhibition facilitates erlotinib  
755 cytotoxicity in lung cancer cells through modulation of endoplasmic reticulum stress. *International*  
756 *journal of oncology* **48**: 2558-2566

757

758 Wei Y, Zou Z, Becker N, Anderson M, Sumpter R, Xiao G, Kinch L, Koduru P, Christudass CS, Veltri  
759 RW, Grishin NV, Peyton M, Minna J, Bhagat G, Levine B (2013) EGFR-mediated Beclin 1  
760 phosphorylation in autophagy suppression, tumor progression, and tumor chemoresistance. *Cell* **154**:  
761 1269-1284

762

763 Wu HB, Yang S, Weng HY, Chen Q, Zhao XL, Fu WJ, Niu Q, Ping YF, Wang JM, Zhang X, Yao XH,  
764 Bian XW (2017) Autophagy-induced KDR/VEGFR-2 activation promotes the formation of vasculogenic  
765 mimicry by glioma stem cells. *Autophagy* **13**: 1528-1542  
766  
767 Yao Z, Fenoglio S, Gao DC, Camiolo M, Stiles B, Lindsted T, Schleiderer M, Johns C, Altorki N, Mittal  
768 V, Kenner L, Sordella R (2010) TGF-beta IL-6 axis mediates selective and adaptive mechanisms of  
769 resistance to molecular targeted therapy in lung cancer. *Proc Natl Acad Sci U S A* **107**: 15535-15540  
770  
771 Ye M, Wang S, Wan T, Jiang R, Qiu Y, Pei L, Pang N, Huang Y, Huang Y, Zhang Z, Yang L (2017)  
772 Combined Inhibitions of Glycolysis and AKT/autophagy Can Overcome Resistance to EGFR-targeted  
773 Therapy of Lung Cancer. *Journal of Cancer* **8**: 3774-3784  
774  
775 Yeo SK, Wen J, Chen S, Guan JL (2016) Autophagy Differentially Regulates Distinct Breast Cancer  
776 Stem-like Cells in Murine Models via EGFR/Stat3 and Tgfbeta/Smad Signaling. *Cancer research* **76**:  
777 3397-3410  
778  
779 Yu HA, Arcila ME, Rekhtman N, Sima CS, Zakowski MF, Pao W, Kris MG, Miller VA, Ladanyi M,  
780 Riely GJ (2013) Analysis of tumor specimens at the time of acquired resistance to EGFR-TKI therapy in  
781 155 patients with EGFR-mutant lung cancers. *Clinical cancer research : an official journal of the*  
782 *American Association for Cancer Research* **19**: 2240-2247  
783  
784 Yu L, Chen Y, Tooze SA (2017) Autophagy pathway: cellular and molecular mechanisms. *Autophagy*: 0

785

786 Yuan J, Zhang N, Yin L, Zhu H, Zhang L, Zhou L, Yang M (2017) Clinical Implications of the  
787 Autophagy Core Gene Variations in Advanced Lung Adenocarcinoma Treated with Gefitinib. *Scientific*  
788 *reports* **7**: 17814

789

790 Zeng X, Zhao H, Li Y, Fan J, Sun Y, Wang S, Wang Z, Song P, Ju D (2015) Targeting Hedgehog  
791 signaling pathway and autophagy overcomes drug resistance of BCR-ABL-positive chronic myeloid  
792 leukemia. *Autophagy* **11**: 355-372

793

794 Zou Y, Ling YH, Sironi J, Schwartz EL, Perez-Soler R, Piperdi B (2013) The autophagy inhibitor  
795 chloroquine overcomes the innate resistance of wild-type EGFR non-small-cell lung cancer cells to  
796 erlotinib. *Journal of thoracic oncology : official publication of the International Association for the*  
797 *Study of Lung Cancer* **8**: 693-702

798

799

800

801

## 802 **Figure Legends**

803 **Figure 1.** Autophagy inhibition resulted in increased osimertinib sensitivity in osimertinib-sensitive  
 804 cells. (A) Fluorescent micrographs of autophagosomes in PC-9GR and PC-9 cells treated with or  
 805 without osimertinib for 24h. Scale bar, 10 $\mu$ m. (B) Western blot showing that high autophagy flux was  
 806 found in PC-9 cells treated with osimertinib. (C) Osimertinib treatment induced autophagy to a much  
 807 greater extent than that of gefitinib in both PC-9 cells and PC-9GR cells. Gefitinib, 10nM in PC-9 cells  
 808 and 4  $\mu$ M in PC-9GR cells; osimertinib, 20nM in PC-9 cells and 10M in PC-9GR cells. The level of  
 809 LC3 was examined using Western blot. (D) MTT assay for PC-9GR and PC-9 cells treated with the  
 810 indicated concentrations of osimertinib for 72h. Experiments were performed in triplicate, and data are  
 811 mean $\pm$ SEM. (E) Ki67 staining of PC-9GR cells treated with osimertinib with or without spautin-1(10  
 812  $\mu$ M). Scale bar, 100 $\mu$ m. Experiments were performed in triplicate, and data are mean $\pm$ SEM. Histogram  
 813 shows the percentages of Ki67-positive cells in the indicated groups (\*p<0.05 by Student's t test) (F)  
 814 MTT assay for PC-9GR cells treated with the indicated concentrations of osimertinib with or without  
 815 rapamycin (500 nM) for 48h. Experiments were performed in triplicate, and data are mean $\pm$ SEM  
 816 (\*p<0.05 by Student's t test). (G) Western blot assessment of PC-9GR cells treated with rapamycin for  
 817 48h.

818  
 819 **Figure 2.** Establishment of osimertinib-resistant cell lines from parental PC-9GR, PC-9, and H1975  
 820 cells. (A) Micrographs of parental and the corresponding resistant cells. Scale bar, 30 $\mu$ m. (B) MTT  
 821 assay for parental PC-9GR, PC-9, H1975 cells and their corresponding resistant cells treated with  
 822 increasing concentrations of osimertinib for 48 hours. Experiments were performed in triplicate, and  
 823 data are mean $\pm$ SEM. Histogram shows IC50 values in the indicated groups (\*\*p<0.01 by Student's t

test). (C) Colony formation assay of resistant and parental PC-9GR, PC-9, and H1975 cell lines. (D) Summary of the gene alterations in each resistant cell lines and parental cell lines detected by whole-exome sequencing.

**Figure 3.** Enhanced autophagy in osimertinib-resistant cells determines osimertinib resistance. (A) Fluorescent micrographs of autophagic vacuoles in parental PC-9GR, PC-9, H1975 cells and the corresponding resistant cells. Scale bar, 10 $\mu$ m. (B) Western blot showing increased LC3-II levels and decreased p62 amounts in resistant cells. (C) MG132 treatment resulted in increased LC3-II levels in resistant PC-9OR3 cells when compared to that of PC-9 cells. (D) Micrographs obtained by transmission electron microscopy showing enhanced autophagosomes in resistant cells compared with parental PC-9GR, PC-9, and H1975 cells. Magnification, 4 $\times$ 10<sup>4</sup>. (E) The level of autophagy flux is increased in PC-9GROR cells. Representative images of mCherry-EGFP-LC3 vector were shown by fluorescent detection. The level of autophagy flux in PC-9GROR cells were increased compared with that in PC-9GR cells. Quantitative analysis of the number of yellow autophagosomes and red autolysosomes. \*\*P < 0.01. (F) MTT assay for parental PC-9GR, PC-9, and H1975 cells and the corresponding resistant cells. Cells were treated with osimertinib with or without autophagy inhibitor, spautin-1 (10 $\mu$ M) for 72 hours. Experiments were performed in triplicate, and data are mean $\pm$ SEM. Histogram shows IC50 values in the indicated groups (\*p<0.05, \*\*p<0.01 by Student's t test).

**Figure 4.** Osimertinib resistant cells show robust stem-cell like properties. (A) Parental and resistant cells were diluted to single cells per well in 6-well low-adhesion plates. Micrographs of spheres formed



846 after 7 days. (B) CD133/CD44 positive cells were detected by flow cytometry using anti-CD133-FITC  
847 and CD44-PE antibodies. Top left and top right quadrants represent CD133 positive populations, while  
848 top right and lower right are CD44 positive populations. The bar chart shows percentages in various  
849 groups (n=3, \*p<0.05 by Student's t test). (C) Western blot showing the expression levels of the  
850 potential stem markers ALDH1 and Sox2 in osimertinib-resistant cells.

851

852 **Figure 5.** Loss of Sox2 and ALDH1 affects stemness and osimertinib resistance. (A) MTT assay for  
853 PC-9OR3 cells transfected with control, Sox2, and ALDH1A1 siRNAs, respectively, treated with  
854 increasing concentrations of osimertinib for 48 hours. Experiments were performed in triplicate, and  
855 data are mean±SEM. Histogram shows IC50 values in the indicated groups (\*\*p<0.01 by Student's t  
856 test). (B) Colony formation and pulmosphere formation assays for assessing the PC-9OR3 cell line after  
857 transfection with control, Sox2, and ALDH1A1 siRNAs, respectively. (C) CD133/CD44 positive cells  
858 were detected by flow cytometry with anti-CD133-FITC and CD44-PE antibodies. The bar chart shows  
859 percentages in various groups (n=3, p<0.05 by Student's t test). (D) Western blot showing the expression  
860 levels of Sox2 and ALDH1 in the PC-9OR3 cell line after transfection with ALDH1A1 and Sox2  
861 siRNAs, respectively.

862

863 **Figure 6.** Beclin 1-mediated, not Atg5-dependent autophagy is critical for stem-cell like properties and  
864 osimertinib resistance. (A) Pulmosphere formation assay for PC-9OR3 cells treated with DMSO or the  
865 autophagy inhibitor spautin-1 (10μM). (B) CD133/CD44 positive PC-9OR3 cells were detected after  
866 treatment with spautin-1 alone or combined with osimertinib. (C) ALDH1A1 and Sox2 levels measured  
867 by Western blot in PC-9OR3 cells after treatment with spautin-1 and osimertinib. (D) Phospho-beclin 1

(Ser93), total beclin1, and Atg5 levels measured by Western blot in parental PC-9 and resistant PC-9OR3 cells. (E) Cell viability of PC-9OR3 cells transfected with control, beclin 1, and Atg5 siRNA, respectively. Experiments were performed in triplicate, and data are mean±SEM. (F) Colony formation and pulmosphere formation assays for PC-9OR3 cells after transfection with control, beclin 1, and Atg5 siRNAs, respectively. (G) CD133/CD44 positive PC-9OR3 cells were detected after transfection with control, beclin 1, and Atg5 siRNAs, respectively, by flow cytometry with anti-CD133-PITC and CD44-PE antibodies. (H) Sox2 and ALDH1 levels were measured in PC-9OR3 cells after transfection with control, beclin 1, and Atg5 siRNAs, respectively. (I) Sox2 and ALDH1 levels were measured in PC-9OR3 cells after transfection with control or beclin 1 siRNAs following with MG132 treatment for 6h. (J) qPCR analysis of mRNA level of Sox2 and ALDH1 after beclin 1 knockdown.

**Figure 7.** Combination of the autophagy inhibitor CQ and osimertinib effectively inhibits the growth of PC-9GR xenografts. (A) PC-9GR xenografts were treated with control, CQ, osimertinib, and combined CQ/osimertinib, for 8 weeks. Tumor sizes were presented as mean±SEM (n=8); n.s, not significant compared with the control group; \*, P<0.001 compared with the control group; †, P<0.01 compared with the control group; ‡, P<0.05 compared with the osimertinib alone group. (B) Body weight were presented as mean±SEM (n=8); n.s, not significant. (C) Representative immunohistochemical staining results for LC3 and Sox2, and hematoxylin-eosin staining for tumor xenografts from nude mice. (D) Whole protein cell lysates were prepared randomly from 3 tumors per group for Western blot to detect the indicated proteins.

**Figure 8.** Enhanced autophagy was found in patients with acquired resistance to osimertinib. (A) A chart

890 showing potential resistance mechanisms to osimertinib in 39 NSCLC patients. More than 50% patients  
 891 developed resistance by yet unknown mechanisms. (B) Immunohistochemical staining results for LC3  
 892 and hematoxylin-eosin staining in paired tumor sections from 5 patients (before osimertinib treatment  
 893 and after osimertinib resistance). Positive staining was seen in patient #1,4 and 5 after osimertinib  
 894 treatment. (C) Overall mutation spectrum of the 5 patients. Different color presents different types of  
 895 baseline mutation. The top bar demonstrated the number of mutations detected in an individual patient.  
 896 The side bar stands for the number of patients harboring the corresponding mutation.

# Figure 1

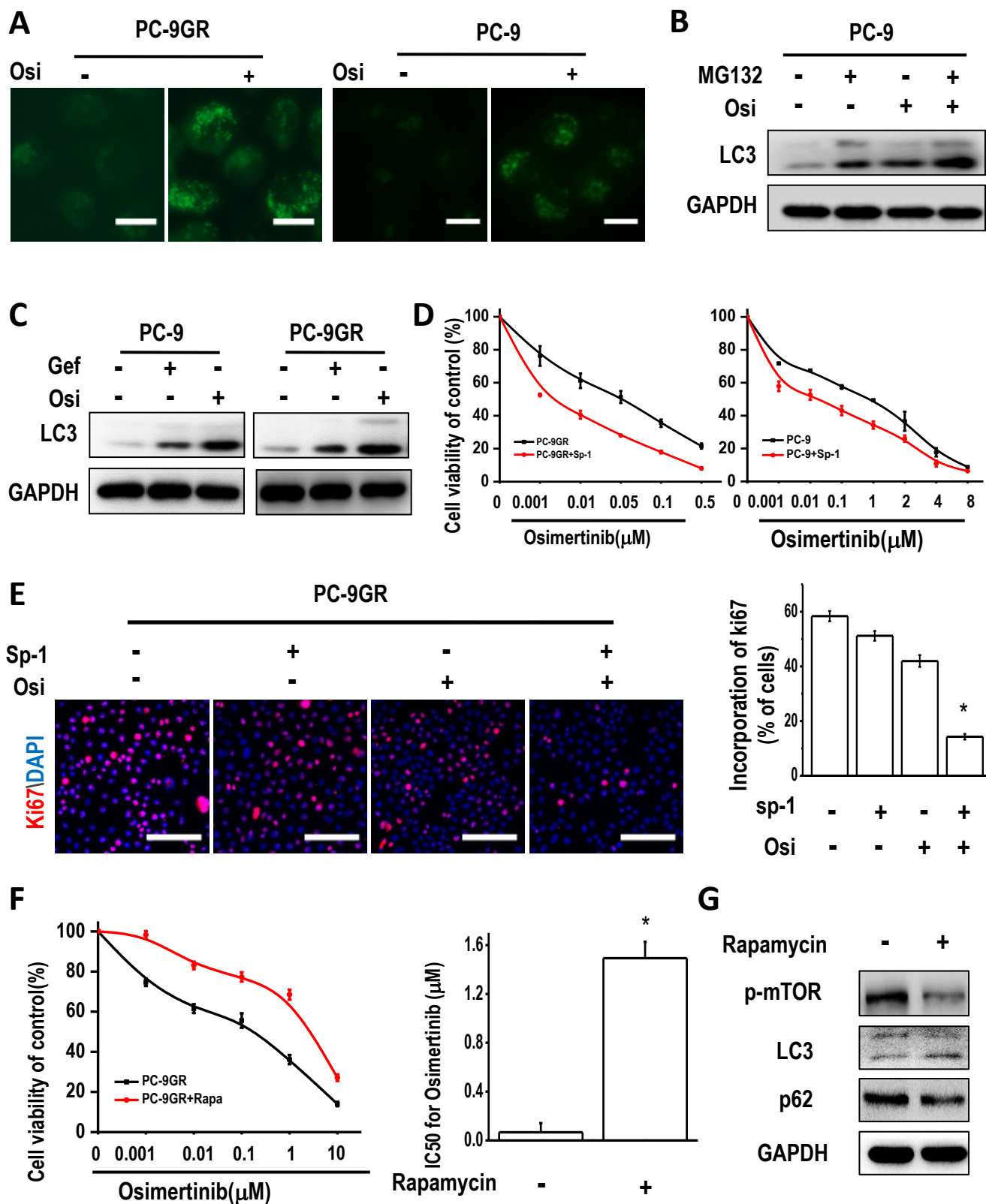
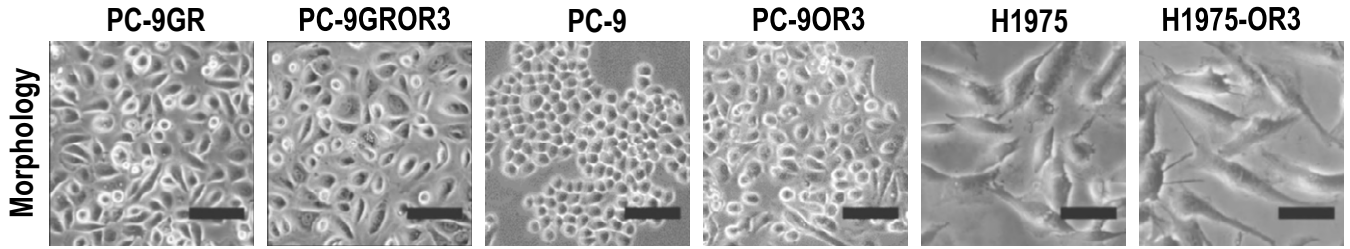
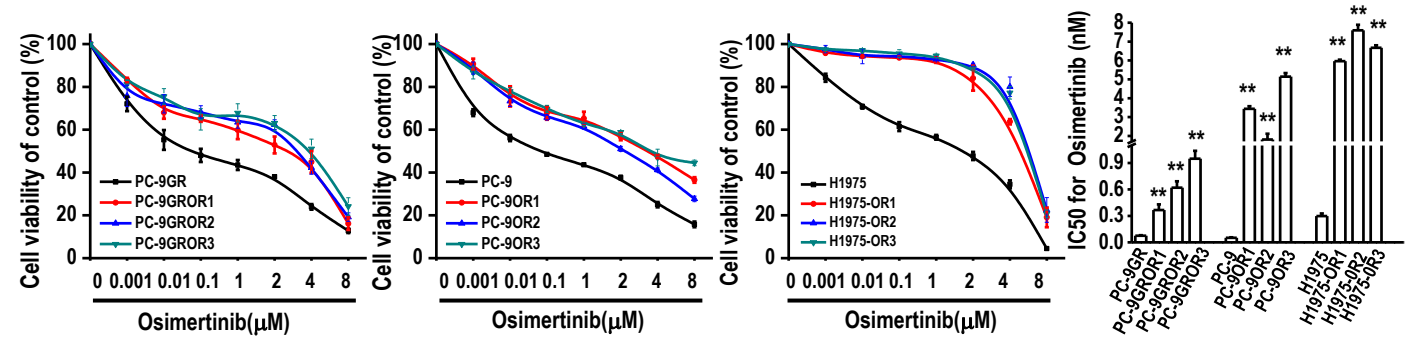


# Figure 2

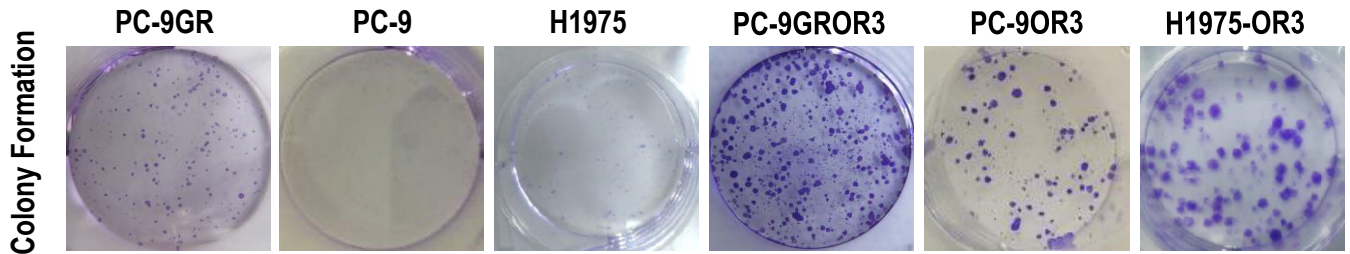
A



B



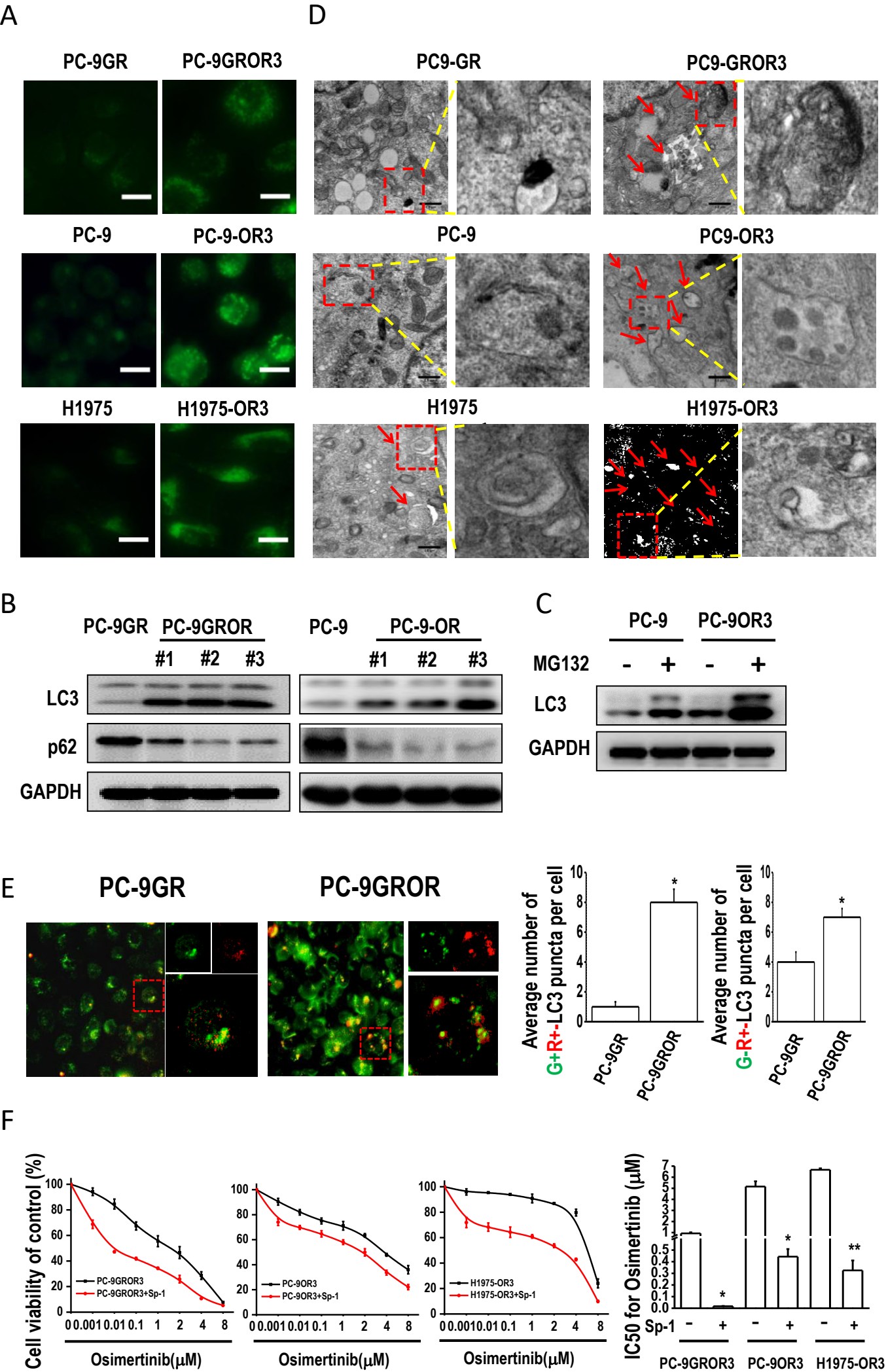
C



D

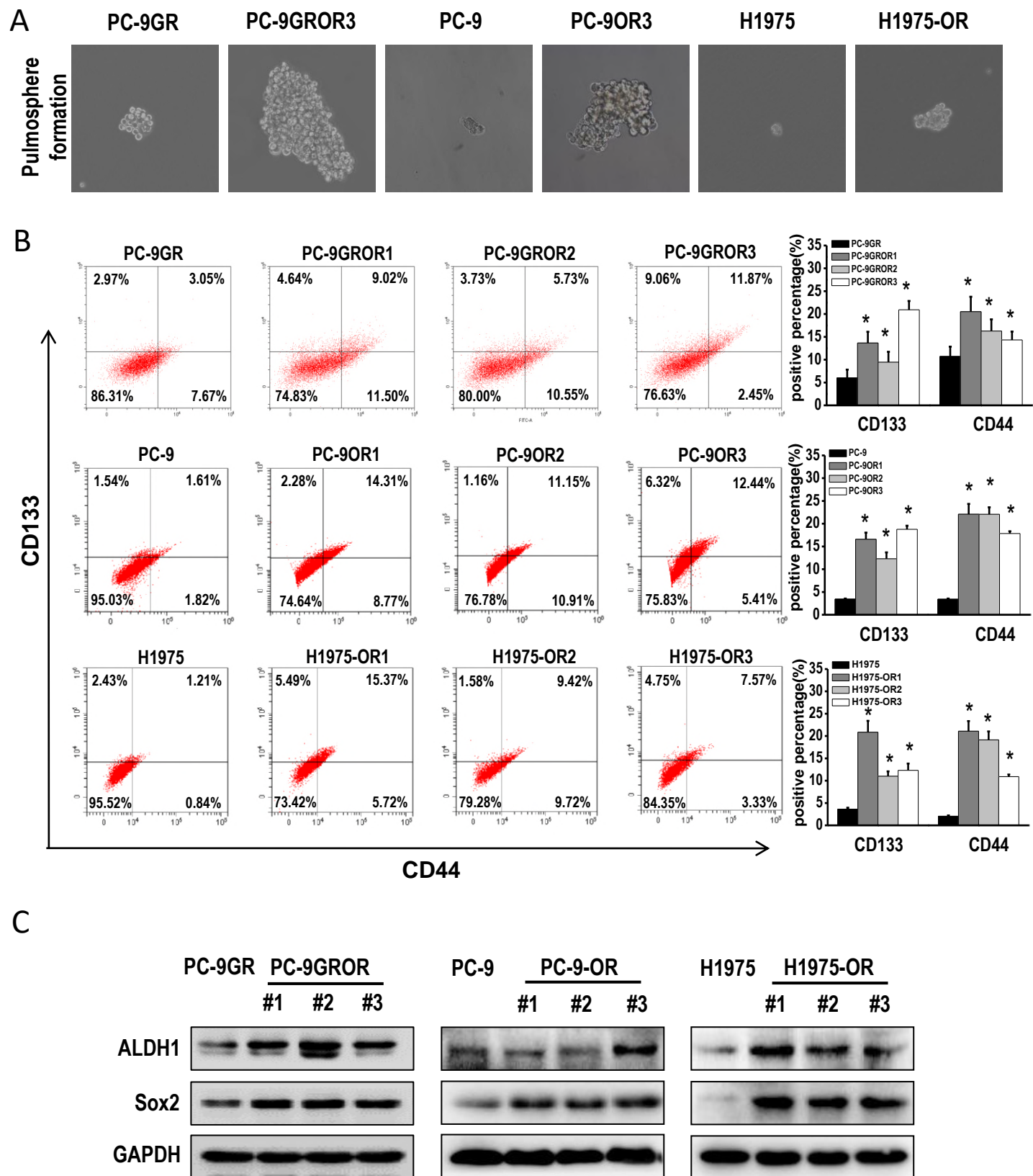
cell lines	Del19	L858R	T790M	EGFR amplification	Met amplification	BRAF amplification
PC-9	+	-	-	-	-	-
PC-9OR1	+	-	-	-	-	-
PC-9OR2	+	-	-	-	-	-
PC-9OR3	+	-	-	-	-	-
PC-9GR	+	-	+	-	-	-
PC-9GROR1	+	-	+	-	-	-
PC-9GROR2	+	-	+	-	-	-
PC-9GROR3	+	-	-	+	-	-
H1975	-	+	+	-	-	-
H1975-OR1	-	+	+	-	+	+
H1975-OR2	-	+	+	-	+	-
H1975-OR3	-	+	+	-	+	-

Figure 3





# Figure 4



# Figure 5

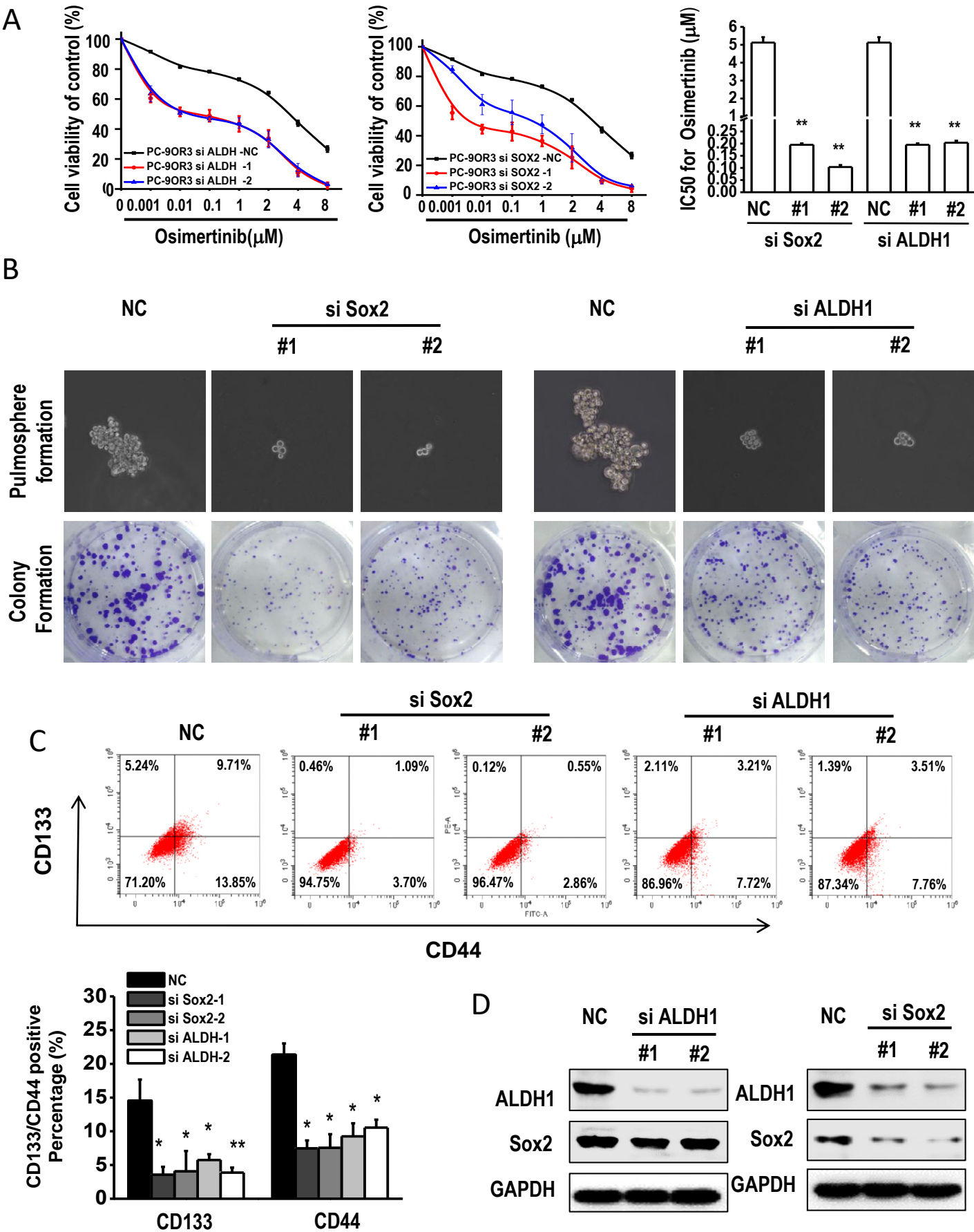




## Figure 6

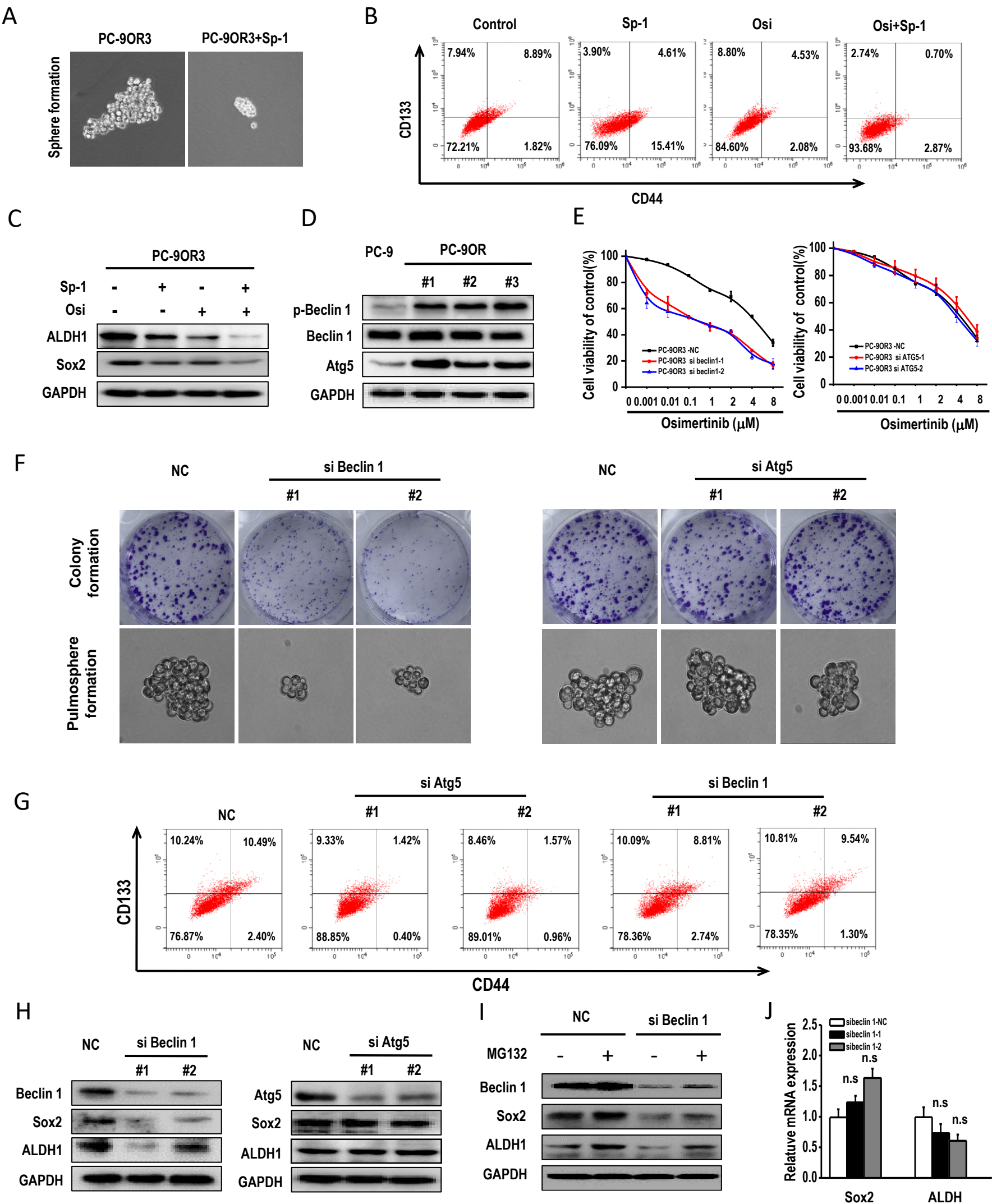
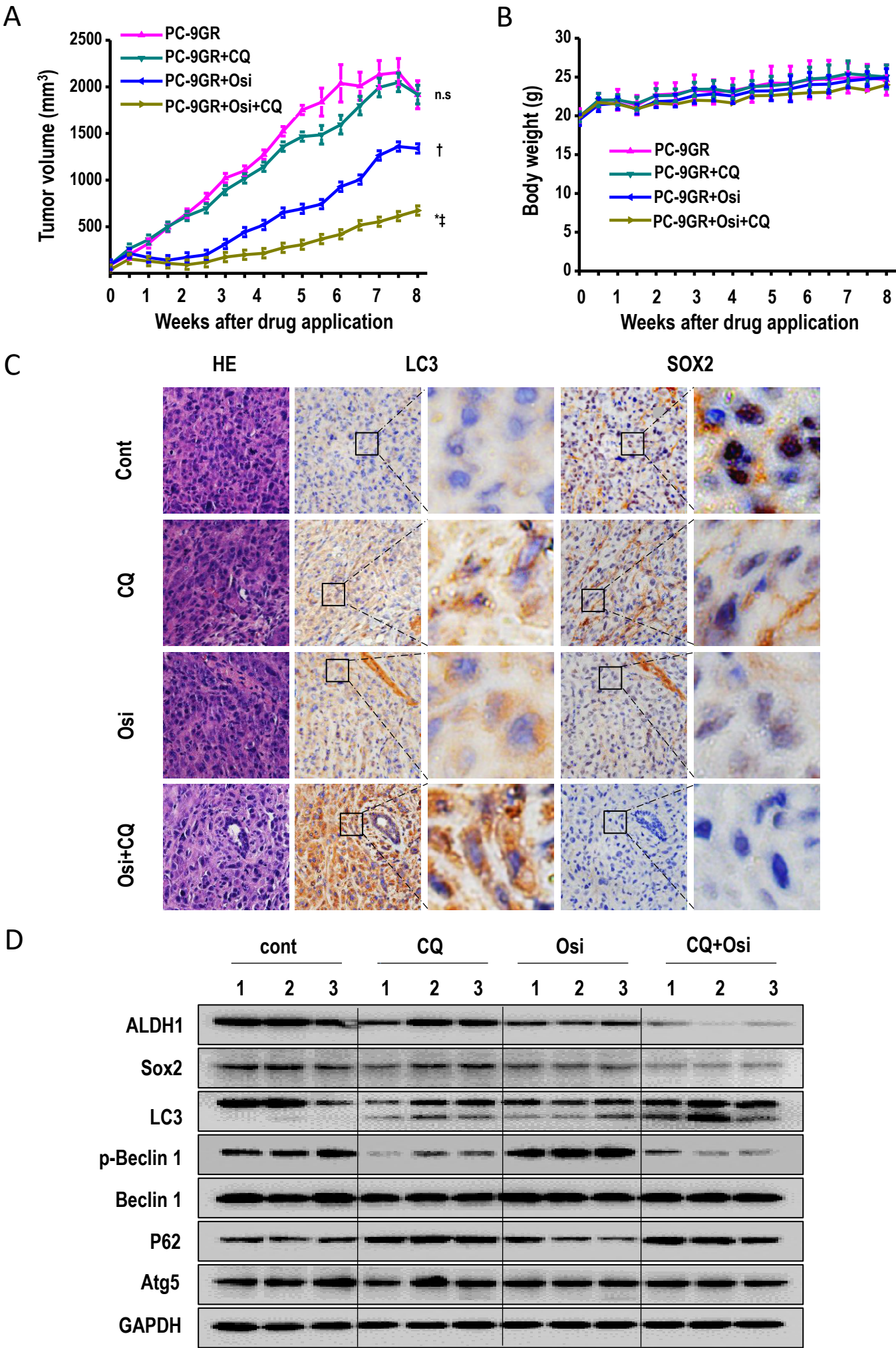
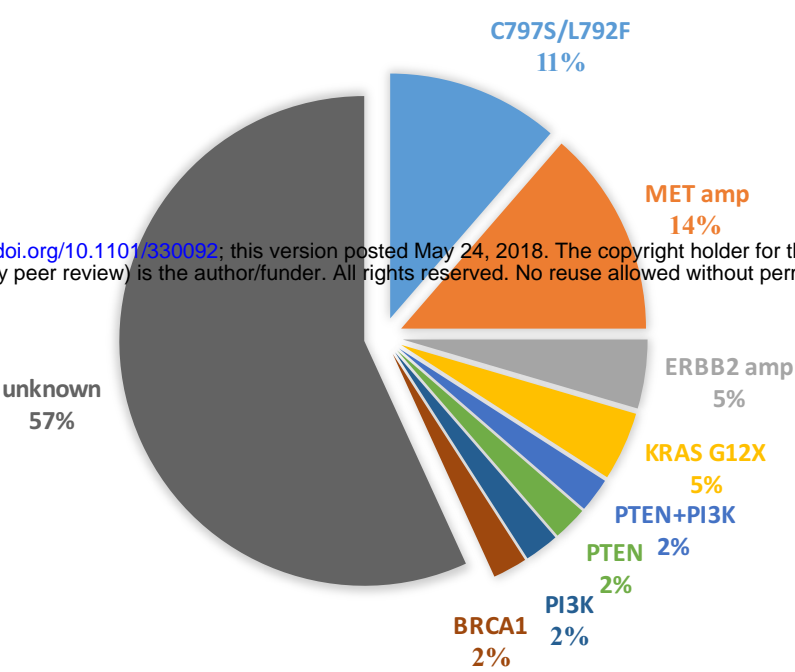


Figure 7

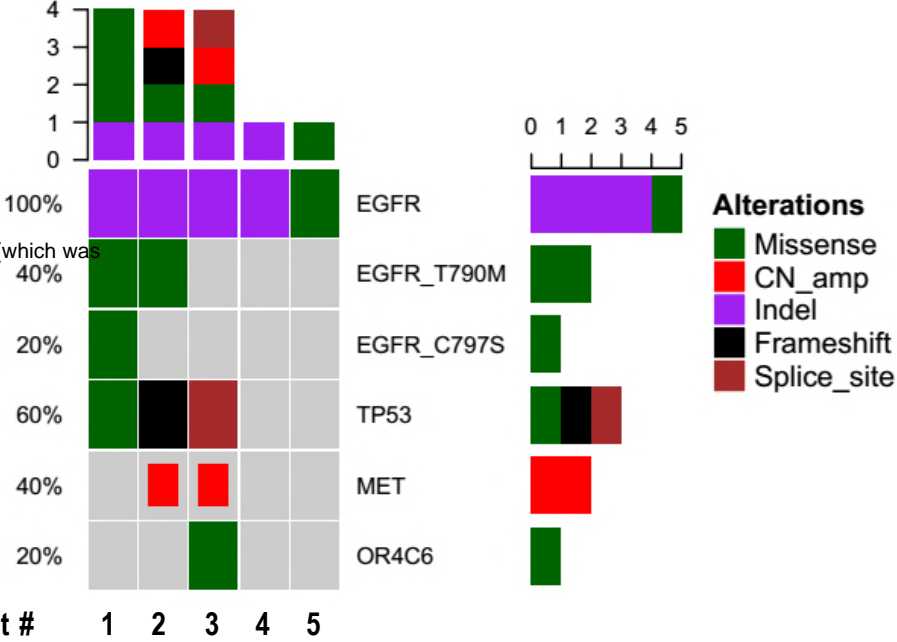




A



C



B

